UNIVERSITÀ DEGLI STUDI DI PALERMO

Dottorato di Ricerca in Biomedicina e Neuroscienze
Dipartimento di Biomedicina e Neuroscienze Cliniche (BioNeC)
SSD BIO/16

Onset of Insulin Resistance in Hippocampal Synapses After Traumatic Brain Injury:
Relevance to Alzheimer's disease and Therapeutic Implications

LA CANDIDATA
Dott. Whitney Franklin

LA COORDINATRICE
Chiar.ma Prof.Felicia Farina

IL CO-TUTOR
Chiar.mo Prof. Giulio Taglialatela

TUTOR
Chiar.mo Prof. Francesco Cappello

CICLO XXXI
ANNO ACCADEMICO 2018/2019

TABLE OF CONTENTS

Disclosure

Publications that resulted from this work:

1. **<u>Franklin W.</u>**, Taglialatela G. "A method to determine insulin responsiveness in synaptosomes isolated from frozen brain tissue." J Neurosci Methods. 2016 Mar 1; 261:128-34.

2. **<u>Franklin W.</u>**, Krishnan B., Taglialatela G. "Onset of chronic synaptic insulin resistance after traumatic brain injury abolishes insulin protection from amyloid beta and tau oligomer-induced synaptic dysfunction in the rat hippocampus." [In Preparation]

Acknowledgements

I would like to thank my mentor, Dr. Taglialatela, for all of his guidance and support over the years, both professionally and personally. I would like to thank both past and present members of Dr. Taglialatela's lab- Dr. Olga Zolochevska, Dr. Claudia Marino, Dr. Salvo Saieva, Dr. David Briley, Wen Ru Zhang, Dr. Michele Comerota, and Dr. Anna Fracassi for their technical and emotional support throughout my time in the lab. An additional thank you to Dr. Balaji Krishnan for his assistance and advice to accomplish all of the electrophysiology experiments.

Guidance and advice for my project from my committee members: Drs. Rakez Kayed, Lee Shapiro, Nicola Abate, Balaji Krishnan, and Giulio Taglialatela.

The UTMB dean Dr. David Niesel, NGP program director Dr. Owen Hamill, past NGP program coordinator Aurora Galvan, and UNIPA Neuroscience program director Dr. Francesco Cappello.

Most importantly, to my family, to whom I owe everything. To my parents, Pam and Darrell, who gave me everything I could ever need, made sacrifices to provide me with the best, helped me to explore and guide me throughout my professional endevours, and their unfailing emotional support through my life and throughout graduate school- I would be lost without you both, and I will never be able to express how grateful and lucky I am to be your daughter. To my devoted husband Jimmy, whos incredible support allows me to follow my dreams without any worries, you crack the whip to keep me focused but you also lighten my life so much with your love and humor. You keep me sane and make even the hardest days worth it to come home to you. I love you.

Abstract

Traumatic brain injury (TBI) is a risk factor for the later development of Alzheimer's disease (AD), although the mechanisms contributing to this increased risk are unknown. Insulin resistance is an additional risk factor for AD whereby decreased insulin signaling increases synaptic sensitivity to amyloid beta (Aβ) and tau, thus contributing to the cognitive decline that characterizes this neurodegenerative disorder. Considering this, I used male Sprague-Dawley rats that underwent a lateral fluid percussion injury (FPI) at acute (2 and 7 days post-injury), intermediate (28 days post-injury), and chronic (3 months post-injury) time-points to investigate whether decreased insulin responsiveness in TBI animals is playing a role in synaptic vulnerability to AD pathology. I was able to detect acute and chronic decreases in insulin responsiveness in isolated hippocampal synaptosomes after TBI. In addition to assessing both Aβ and tau binding on synaptosomes, I performed electrophysiology at the intermediate and chronic time-points to assess the dysfunctional impact of Aβ and tau oligomers as well as the protective effect of insulin. While I found no difference in binding or degree of LTP inhibition by either Aβ or tau oligomers between SHAM and TBI animals, I did find that insulin treatment was able to block oligomer-induced LTP inhibition in SHAM animals but not in TBI animals. Since insulin treatment has been discussed as a therapy for AD, this gives valuable insight into therapeutic implications of treating AD patients based on a patient's history of associated risk factors.

Introduction

A. Alzheimer's Disease

<div align="center">

I.   Overview and Pathology

</div>

Alzheimer's disease (AD) is a devastating neurodegenerative disorder that was first reported in 1906[1,2]. It is the most common form of dementia, affecting over 47 million people worldwide[3,4]. Over 5 million of those affected are Americans which costs the U.S. more than $200 billion each year[1]. This doesn't even take into account the hours put in by unpaid caregivers. As these numbers are estimated to triple by 2050[1], this would bankrupt our healthcare system unless we can find a way to combat these growing numbers of AD cases.

The cause of the disease is still unknown, and there is still currently no "disease-modifying" cure. There are currently only treatments for the symptoms which include amnesia, aphasia, agnosia, apathy, language alterations, loss of spatial orientation, and loss of executive functions[5,6]. There are currently five pharmacological treatments that are FDA approved which all act on either the cholinergic or glutamatergic circuits affected in AD to help alleviate symptoms[1].
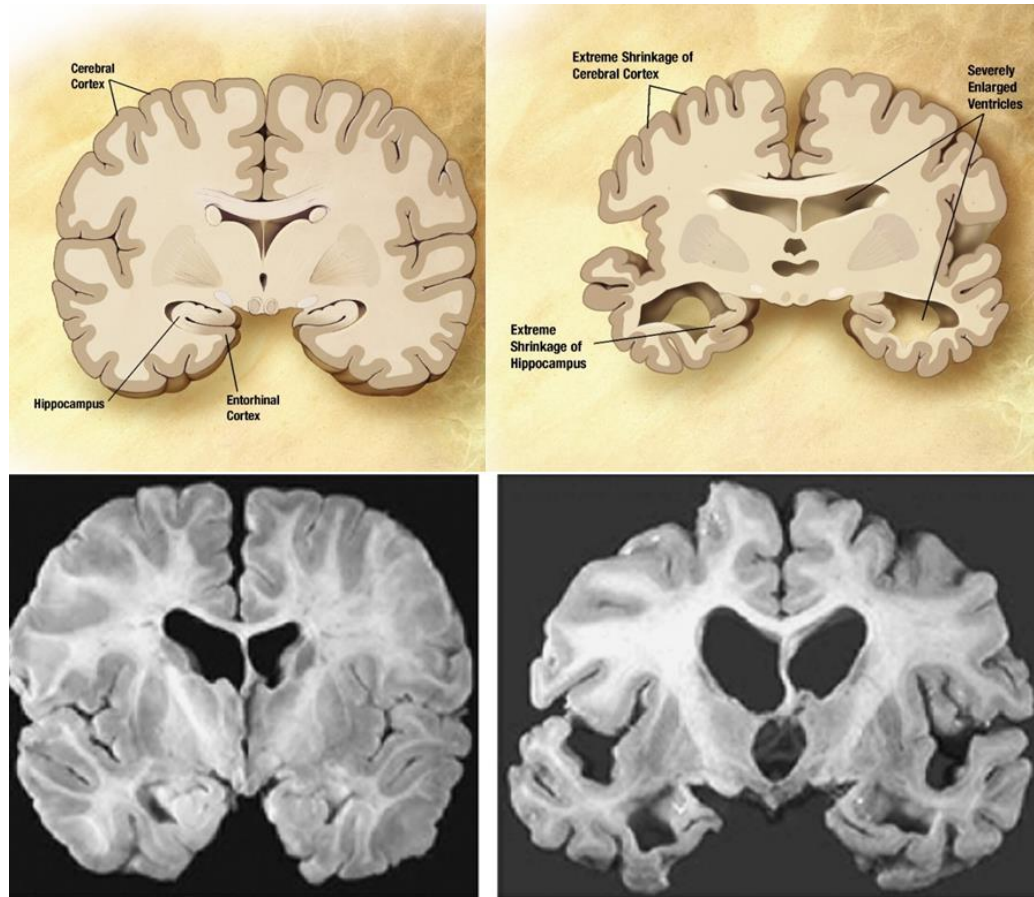
Figure 1: Coronal section of postmortem human brain. Brain slices from an elderly non-demented individual on the left compared with that of a patient with AD on the right, demonstrating hippocampal and cortical shrinkage along with enlarged ventricles in AD [Modified from Figure 1 Yaari et al, 2007].

Histopathologically, AD patients present with neuronal loss in the cortex and hippocampus, evident by hippocampal shrinkage and ventricle enlargement[7] (Figure 1). Protein deposition is found by the presence of extracellular plaques mainly consisting of amyloid beta (Aβ) peptide and intracellular inclusions of neurofibrillary tangles (NFT) composed of hyperphosphorylated tau[8].

Aβ is a cleavage product of amyloid precursor-protein (APP). APP is a membrane spanning protein that is cleaved by secretases resulting in either a detrimental amyloidogenic or non-toxic non-amyloidogenic producing pathway depending on the specific secretases involved (Figure 2A). For the non-amyloidogenic process, cleavage of APP by α-secretase will produce sAPPα and a

remaining c-terminal membrane-bound product (C83) that undergoes further cleavage by γ-secretase to produce p3 and the amyloid intracellular domain (AICD). However, in the amyloidogenic processing pathway, β-secretase beta-site amyloid precursor protein–cleaving enzyme 1 (BACE-1) cleaves rather than α-secretase, resulting in sAPPβ and a different C-terminal fragment (C99). C99 is then further processed by γ-secretase cleavage to produce AICD and the potentially toxic Aβ peptide which is then released into the space outside the neuron and can begin to aggregate[5,9]. The length of the Aβ peptide can vary from 36-43 amino acids[10]. However, the two primary forms associated with AD are 40 and 42 amino acids in length. Aβ42 has a higher propensity for aggregation and is therefore thought to be the more toxic species[5]. In the amyloid

hypothesis for AD, it is suggested that there is an accumulation of Aβ which induces an "Aβ driven cascade" that triggers the disruption and destruction of nerve cells leading to the dementia[3].

Tau proteins belong to the microtubule-associated proteins (MAP) family and are mainly found in neurons. They are part of the cytoskeletal network and have an important role in microtubule assembly and stabilization. The tau gene contains 16 exons, many of which are constitutively expressed in all of the isoforms. There are 6 isoforms in humans that differ in the addition or the omission of exons 2, 3, and 10 (Figure 2B). Exon 2 and 3 are found towards the N-terminus and thus tau isoforms can be designated 0N, 1N, or 2N based on the number of inserts added. Exon 10 is found in the C-terminus of tau and is named 4R for 4 repeats when it is present and 3R designating 3 repeats when exon 10 is absent[11]. The different isoforms vary in localization,
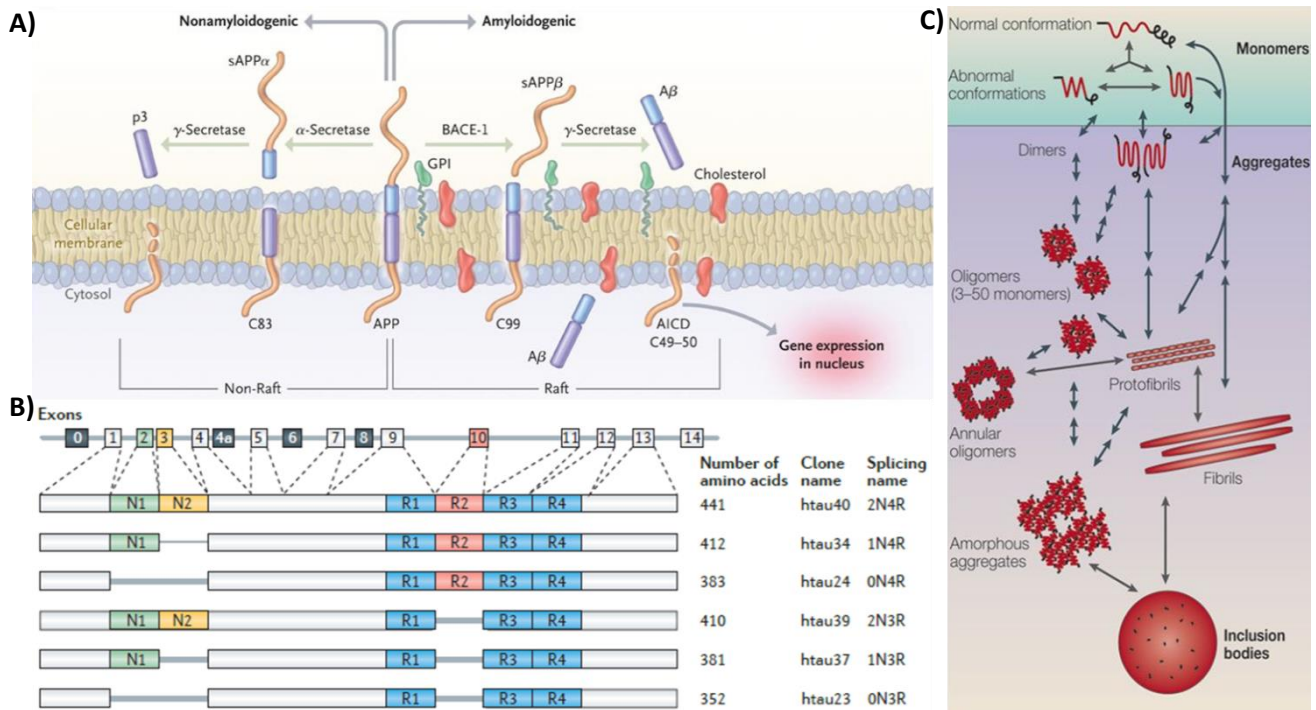
Figure 2: Schematic Representations of APP and Tau Processing and Aggregation. A) Processing of amyloid precursor protein (APP) in nonamyloidogenic and amyloidogenic pathways [Adapted from Figure 1 Querfurth et al., 2010]. B) The human MAPT gene and the splice isoforms of tau in the human brain [Modified from Figure 1 Wang et al., 2016]. C) Aggregation pathways leading to various conformational species including oligomers, annular oligomers, protofibrils, fibrils, and larger aggregates including plaques and tangles. [Adapted from Figure 3 Ross et al., 2005].

efficiency in microtubule assembly, and aggregation potential. The C-terminus of the protein is mainly the site of phosphorylation and hyperphosphorylation, among other post-translational modifications, which can cause tau to aggregate as well[12].

Both amyloid beta and tau have been shown to follow similar abnormal aggregation paths (Figure 2C) whereby monomers will begin to aggregate together forming soluble oligomers. Oligomers then clump further with either additional monomers or oligomers to grow and become insoluble protofibrils and fibrils[13]. Eventually, other proteins and cellular material are added, and these increasingly insoluble entities combine to become the well-known plaques and hyperphosphorylated tangles that are characteristic of AD[14].

Previously, it was thought that plaques and fibrils might cause all of the damage to neurons that is seen in AD. It has become increasingly evident that it is the oligomeric aggregates of both Aβ and tau that contribute to the synaptic dysfunction that precedes the cognitive decline seen in AD[15,16]. Furthermore, it has been shown that oligomer toxicity is induced by the conformation, regardless of the differing primary structure and sequence of the peptides comprising these oligomers[17,18]. Thus, both Aβ and tau oligomers have been shown to accumulate at synapses[19] and induce disruptive synaptic alterations (Figure 3). Aβ oligomers can accumulate at the synapse[20], are capable of inducing changes in the composition, shape, and density of the synapse[21,22], can inhibit both early and late phase LTP[23,24], and can disrupt calcium dynamics and calcium-dependent signaling[23,25,26]. Tau also demonstrates these characteristics where it has been seen internalizing into neurons[16] and also inhibiting LTP in its oligomeric aggregation state[15]. It is believed that synaptic dysfunction driven by these oligomers underlies the initiation and progression of AD[27,28].
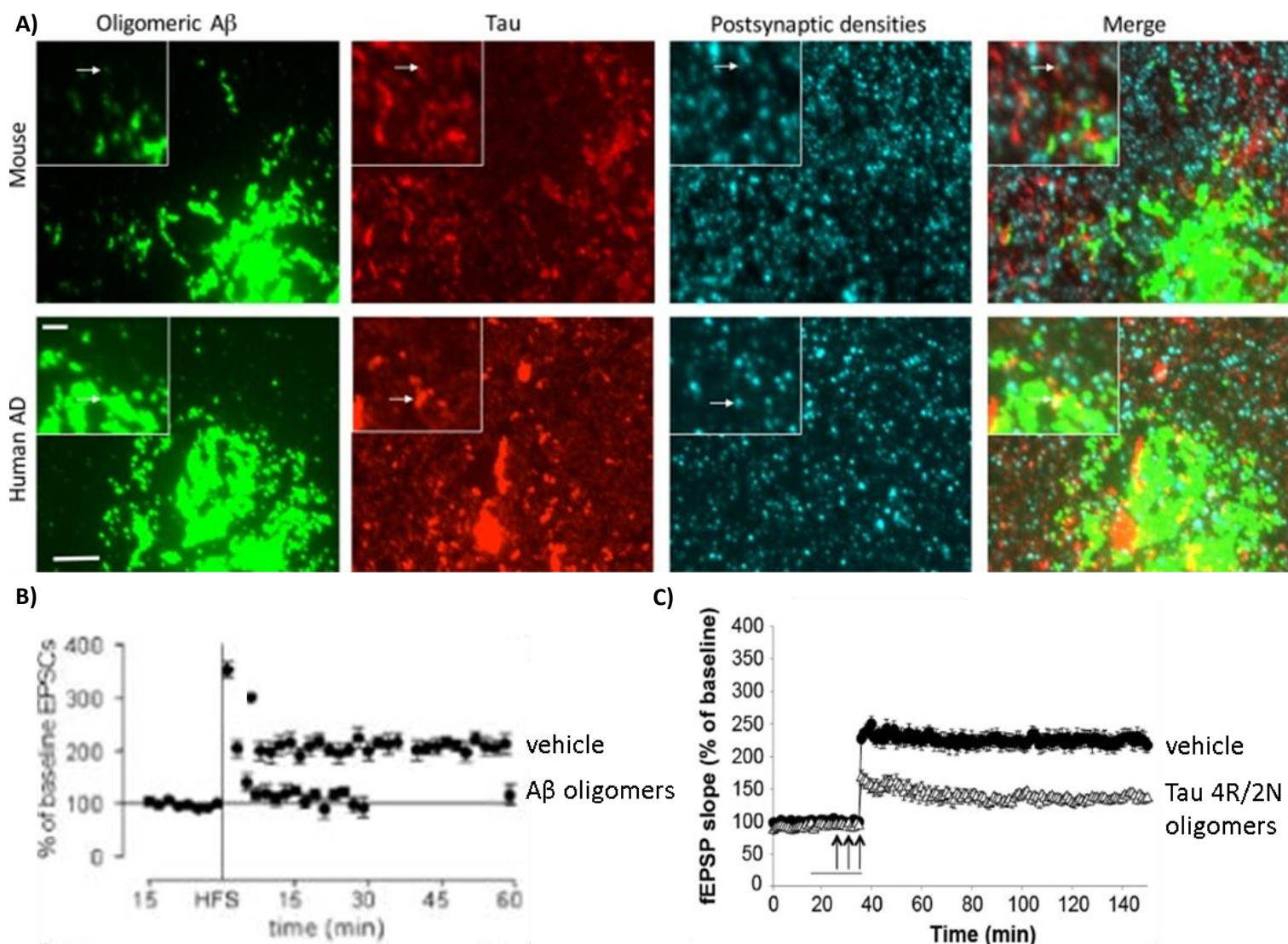
Figure 3: Aβ and tau oligomers bind to synapses and inhibit LTP. A) Immunofluorescent images demonstrating co-aggregation and localization (arrows) of Aβ and tau at synapses in an AD mouse model (APP/PS1 mice also expressing human wild-type tau) (top) and human AD brain (bottom) using the array tomography technique. Scale bars represent 5 µm in large panel and 2 µm in inset [Adapted from Figure 2 Spires-Jones et al., 2017]. B) High-frequency synaptic stimulation (HFS)-induced expression of long-term potentiation (LTP) is inhibited in the hippocampus of rat brain slices treated for 1 hr with 0.5μM oligomeric Aβ compared to vehicle [Modified Figure 2 Dineley et al., 2010]. C) HFS-induced expression of LTP is reduced in the hippocampus of mouse brain slices perfused with 2.29 μg/ml oTau 4R/2N versus 20 minute incubation with vehicle [Adapted from Figure 1 Fá et al., 2016].

II.   Risk Factors

Sporadic AD (sAD) is complex and heterogenous and is responsible for >95% of all AD cases[1,29]. There is a high disease comorbidity with sAD[29] and a large variety of factors that increase the risk of developing sAD[4] (Figure 4).

Some of these risk factors are innate such as age, family history, and APOE genotype. Other risk factors are due to lifestyle and/or are event-related such as type 2 diabetes (T2DM)[30–32], central insulin resistance[33], traumatic brain injury (TBI)[34–36], mitochondrial dysfunction[37,38], neuroinflammation[39], obesity[30], smoking, and sleep deprivation. While we cannot control innate factors, event-related risk factors offer an opportunity for us to decrease the growing number of AD patients.
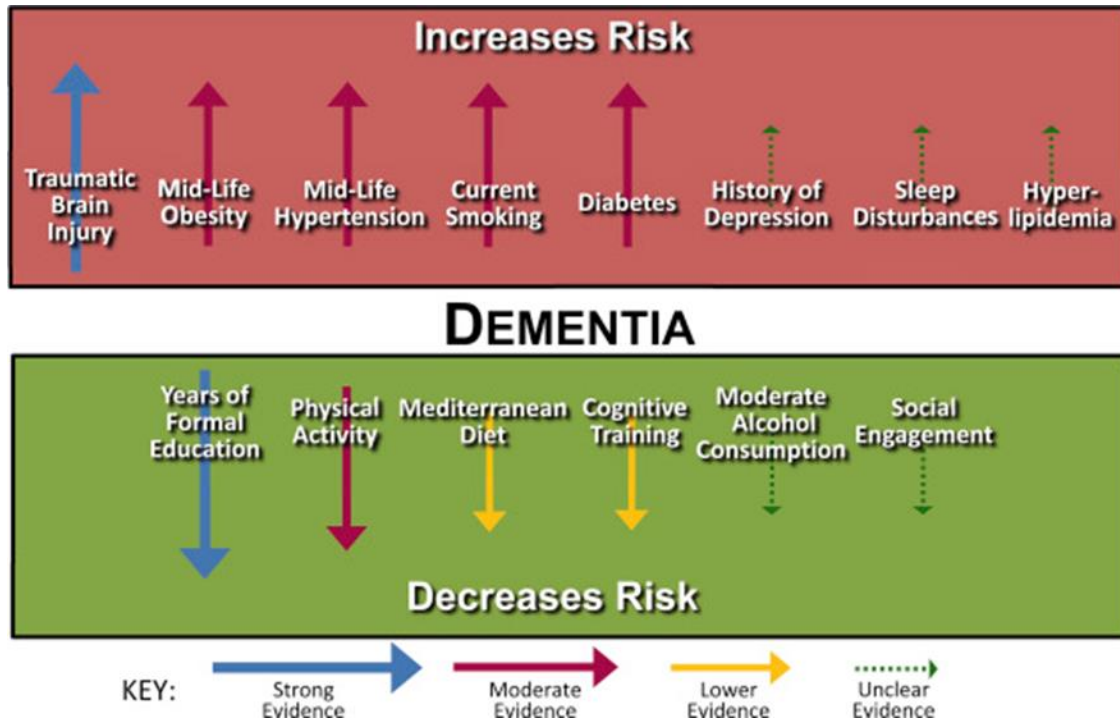
Figure 4: Strength of evidence on risk factors for dementia. Modified from Figure 2 Baumgart et al., 2015.

III.   Insulin and AD

The insulin receptor (IR) is a tyrosine kinase receptor that autophosphorylates and can only be phosphorylated in the presence of its substrate, insulin. It's located in the periphery as well as the central nervous system. In the CNS, it is abundant at synapses in both the hippocampus and cerebral cortex. IRs are involved in glucose metabolism in the periphery but have more diverse functions in the brain including synaptic activities required for learning and memory[40,41].

Since insulin signaling is involved in learning and memory processes as well as synaptic health, it's unsurprising that disruptions in this important pathway have been linked to AD. In addition to T2DM being a risk factor for AD[30–32], cerebral glucose metabolism is reported to be decreased in AD[29]. What's more, even in AD patients without diabetes, the hippocampus exhibits insulin resistance shown by decreased insulin signaling and insulin-like growth factor (IGF) signaling response versus cognitively normal people with doses of 1nM of insulin and IGF-1 that could not be overcome by a 10nM dosage stimulation[42].

Additionally, the protective effects of insulin on Aβ-oligomer binding and destruction at the synapse has been reported when looking at hippocampal neuronal cultures. In work published by De Felice, they showed with immunocytochemistry that Aβ-oligomers bind to synapses and cause synaptic loss that can be inhibited with the addition of insulin. They went on to show that disruption in the insulin receptor function by pharmacologically inhibiting the tyrosine kinase activity of the receptor abolished the ability of insulin to block Aβ oligomer binding[43]. This demonstrated that IR function is needed for this protection rather than insulin acting as a competitor on Aβ binding sites as an explanation for the decreased oligomer binding.

Conversely, they also showed that application and binding of Aβ oligomers caused a loss of insulin receptor surface expression on dendrites and a loss of autophosphorylation capacity of the

receptor[40]. This showed how physiological insulin and pathological Aβ-oligomers negatively regulate the abundance of each other's binding sites.

In addition to these molecular studies, insulin and insulin-sensitizing therapy has been shown to be effective for cognition and behavior in both mouse models of AD as well as in patients with mild cognitive impairment (MCI) or early AD[43–46].

All of this evidence strongly indicates the existence of an intimate relationship between synaptic insulin responsiveness and neuronal sensitivity to AD neuropathology.

B. Traumatic Brain Injury

I.　　Overview

Each year, there is an incidence of roughly 2.7 million traumatic brain injuries in the US alone[47,48]. There are a wide range of effects and complications as a consequence of TBI[49] (Figure 5). There is disruption and dysfunction in the vascular system that leads to a variety of problems with the blood brain barrier (BBB), blood flow, and autoregulation. In addition, there are increases of calcium influx resulting in calcium overload. This disrupts mitochondrial function and allows for the generation of reactive oxygen species (ROS). Moreover, there are neuroinflammation consequences that lead to chronic microglia activation which is damaging to the cell. All of these effects are happening concurrently, interacting with and, in some cases, exacerbating each other all leading to a long list of short-term and long-term deficits including the possibility of AD. Even though all of these disruptions and consequences are known to occur, the exact mechanisms contributing to the increased risk of AD after TBI are unknown.
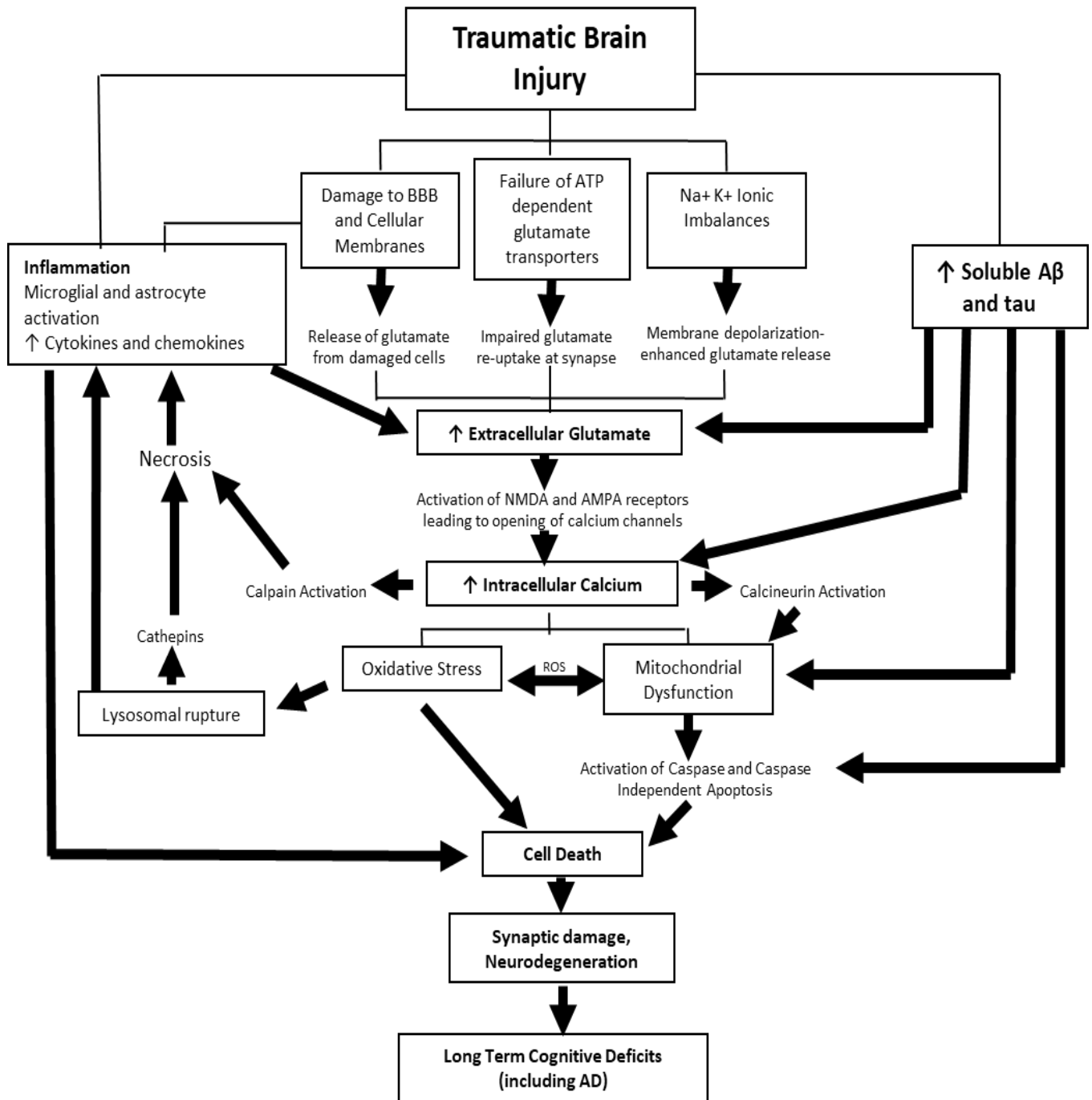
Figure 5: Consequences of traumatic brain injury. Molecular alterations after TBI leading to various acute and chronic diseases and consequences.

II. Alzheimer's disease Consequence

TBI-induced dementia, in particular, is becoming a more central concern as the cost and incidence of AD continue to rise without any effective treatments. There is a dose-response relationship whereby the risk for dementia increases with the severity and number of injuries, but a single moderate or severe injury can still increase the risk of developing dementia diseases.

There are several things that have been postulated and investigated to contribute to the increased susceptibility to AD after TBI. Among these are the presence of the APOE 4 allele (which can increase your chance of generating AD after TBI by 10-fold), phosphorylated tau, and accumulating Aβ after TBI[39,50]. The accumulation of Aβ plaques that has been seen in about 30% of TBI cases in humans[51–53] has been thought to possibly correlate with many things, including elevated soluble Aβ levels after TBI[36], increased Aβ42:40 ratio[52,54], increase in APP processing since both APP[55] and β-secretase concentration have been shown to increase after TBI[53,56–58], and/or decreased Aβ clearance from the brain. However, the increase in soluble Aβ oligomers, APP, and β-secretase seen after TBI is transient whereby there is an increase followed by a decrease to normal levels within just a few days[54]. This acute accumulation therefore could not account for the susceptibility to AD since the patients do not generate dementia within a short time span. Rather, there is a long-term susceptibility causing the patient to be more likely to develop Alzheimer's decades down the road. Ergo, the systemic alteration linking the two diseases must be one that is chronic.

Molecular dysfunction	TBI (clinical and experimental)	AD (human brain and transgenic mouse model)
Impaired synaptic plasticity ↓LTP ↑LTD	Albensi et al., 2000; Scheff et al., 2005	Oddo et al., 2003; Trinchese et al., 2004
Impaired glutamate transport ↓GLAST/EAAT1 ↓GLT-1/EAAT2	Rao et al., 1998; van Landeghem et al., 2006; Yi and Hazell, 2006	Masliah et al., 1996; Li et al., 1997; Scott et al., 2011
↑NMDA receptor activation	Palmer et al., 1993	Revett et al., 2013
Intracellular calcium dysregulation	Sun et al., 2008; Saatman et al., 2010	See review Supnet and Bezprozvanny, 2010
Mitochondrial dysfunction	Xiong et al., 1997; Gilmer et al., 2009	Dragicevic et al., 2010; Reddy et al., 2010
Oxidative stress	Ansari et al., 2008; Cheng et al., 2012	Ansari and Scheff, 2010
Calcineurin activation	Kurz et al., 2005a,b	Liu et al., 2005; Wu et al., 2010
Calpain activation	Vosler et al., 2008; Saatman et al., 2010	Trinchese et al., 2008; Ferreira, 2012
Apoptosis	Minambres et al., 2008; Stoica and Faden, 2010	Castro et al., 2010; Rohn, 2010
Caspase-3 activation	Clark et al., 2000; Stone et al., 2002; Abrahamson et al., 2006; Walker et al., 2012	Tesco et al., 2007; see review Castro et al., 2010; Rohn, 2010
↑BACE1 level and activity	Blasko et al., 2004; Loane et al., 2009; Walker et al., 2012	Fukumoto et al., 2002; Holsinger et al., 2002; Sun et al., 2002; Tyler et al., 2002; Tesco et al., 2007; Cole and Vassar, 2008
↓GGA3 and GGA1 adaptor proteins	Walker et al., 2012	Tesco et al., 2007; Walker et al., 2012
Inflammation and chronic microglial activation	Ramlackhansingh et al., 2011; Acosta et al., 2013	Cagnin et al., 2001; Heneka et al., 2005; Schindowski et al., 2006; Parachikova et al., 2007; Garwood et al., 2010; Ferretti et al., 2012

Table 1: Common pathophysiological mechanisms in TBI and AD. Adapted from Table 2 Walker et al., 2013.

In addition to the Aβ and tau-related changes, there are also several pathophysiological mechanisms that are shared between the two diseases that have been described and investigated including problems with synaptic plasticity, calcium dysregulation, oxidative stress, etc[50] (Table 1). However, all of these have fallen short in finding effective therapies that help alleviate this TBI/AD risk factor connection.

III. Insulin and TBI

There are a multitude of consequences after TBI that suggest that normal insulin functioning can affect TBI recovery and that disruptions may be playing a role in the consequences. Several groups have reported hyperglycemia after TBI and found that uncontrolled blood glucose levels lead to a poorer outcome and recovery[59,60]. Moreover, previous reports have also found an increased mortality after head injury in people with T2DM[61]. While one group has reported acute decreased insulin signaling in the CNS after TBI[62], no studies have investigated TBI-driven insulin resistance at the synapses, particularly in relation to synaptic vulnerability to Aβ and tau.

Aim Of The Dissertation

Traumatic brain injury (TBI) increases the risk of developing Alzheimer's disease (AD) later in life through unknown mechanisms[34–36,50]. Synaptic dysfunction stemming from the interaction and binding of toxic amyloid beta (Aβ) and tau oligomeric species to the pre- and post-synapse is an early event in AD that leads to the cognitive decline that characterizes this disease[16]. Since insulin signaling plays a role in synaptic health and function, disruption of this pathway due to insulin resistance has been implicated in the susceptibility of the synapse to AD pathology[40,43].

The aim of this dissertation is to investigate an altered susceptibility of the synapses to AD pathology in relation to TBI-induced changes in signaling and support systems to give novel insights into the link between the two conditions. My central hypothesis is that TBI promotes insulin resistance at the synapse resulting in increased synaptic sensitivity to the dysfunctional effects of Aβ and tau oligomers. I addressed my central hypothesis with two specific aims. In my first aim, I confirmed that TBI alters insulin responsiveness at the synapse by temporally characterizing hippocampal synaptic insulin responsiveness using an *ex vivo* stimulation method. In my second aim, I tested the hypothesis that synaptic vulnerability to the effects of Aβ and tau is increased after TBI. I addressed this aim by utilizing *ex vivo* binding methods with flow cytometry and ELISA analysis to specifically determine any binding alterations. I additionally performed electrophysiology to investigate changes in functional susceptibility to the oligomers.

This research will contribute to understanding mechanism(s) underscoring the increased risk linking the two diseases, which is critical to develop effective interventions to reduce the incidence of AD in TBI subjects. Additionally, this work further illustrates the importance of considering a prior history of associated risk factors and how these may impact the efficacy of particular treatments that are being investigated for AD in the general population.

Experimental Approach

A. Materials and Methods

Animals

Male Sprague-Dawley rats were utilized for the traumatic brain injuries and subsequent experiments in this study. All rats were 2-4 months old (300-450 grams) at the time of surgery/injury. All experimental protocols involving animals in this study were approved by Institutional Animal Care and Use Committee of the University of Texas Medical Branch. Animals were housed under USDA standards (12:12 hour light dark cycle, food and water ad libitum) at the UTMB vivarium. After the designated amount of time after surgery/injury, the rats were sacrificed by isoflurane overdose and decapitated. The brains were quickly removed, dissected into major regions (frontal cortex, parieto-occipital cortex, hippocampus, midbrain, and cerebellum) and opposing hemispheres ("ipsilateral" referring to the brain hemisphere that underwent the craniotomy in the lateral FPI procedure and "contralateral" for the opposite hemisphere), snap frozen, and stored at −80 °C until ready for further analysis.

An adipocyte-specific ecto-nucleotide pyrophosphate phosphodiesterase (ENPP) over-expressing transgenic mouse model of metabolic syndrome and systemic insulin resistance (IR), AtENPP1-Tg, was used to confirm the validity of the *ex vivo* insulin responsiveness assay. This mouse model has previously been shown to present with marked synaptic insulin resistance[63]. Samples from an adult male AtENPP1-Tg mouse that had been fed with high-fat chow (60% calories from fat – 37.1% saturated) for 12 weeks and a C57Bl/6J (wild-type) mouse that had been fed a regular chow diet (4% calories from fat) as previously described in Sallam et al., 2015 were graciously donated by Dr. Nicola Abate.

Parasagittal Fluid-Percussion Injury

For laboratory models used to induce TBI, there are those that induce either static or dynamic trauma. Dynamic models can induce impact injury through penetration, closed head injuries, acceleration, and direct brain deformation[64]. The TBI model that was used for these experiments is a dynamic model of direct brain deformation impact injury called fluid percussion injury (FPI).

This model of TBI is one of the most widely used and established models. First, a craniotomy is performed to expose part of the brain where fluid pressure will later be applied. The position, lateral or midline, of the craniotomy can be altered to fit the type of brain injury classification desired: focal versus diffuse.
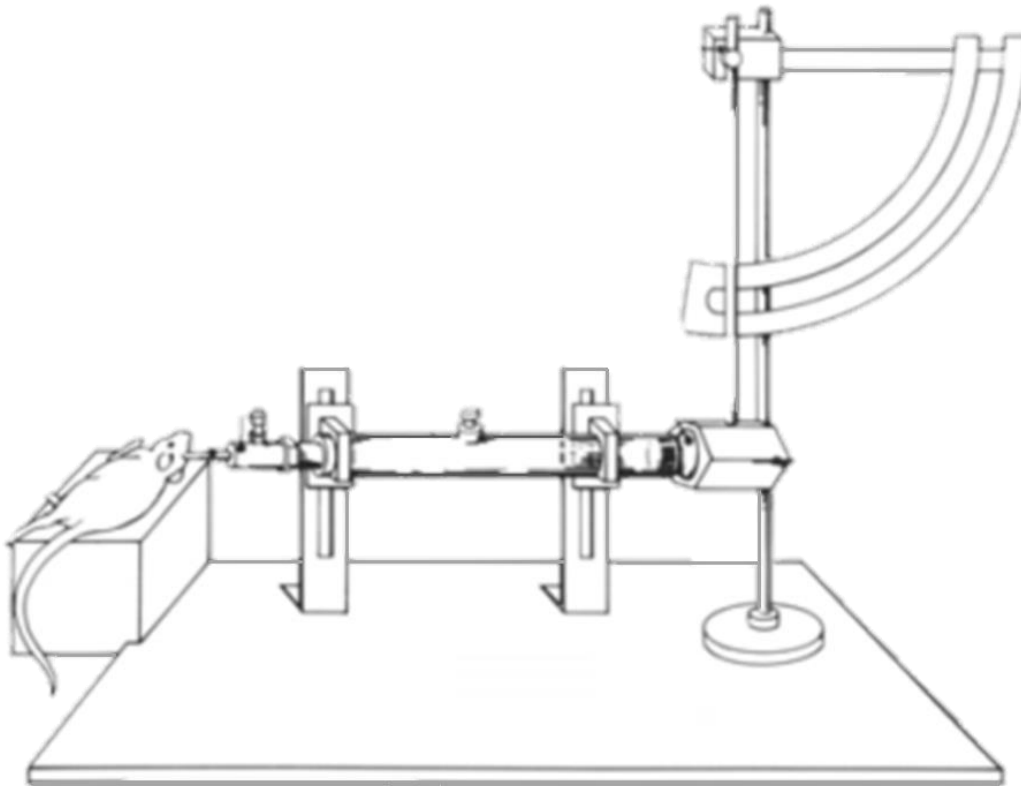
Figure 6: Schematic of fluid-percussion traumatic brain injury model.

The animal's craniotomy site is then connected to the transducer end of the injury device. The pendulum of this device is lifted to a specified height that corresponds to the intensity of injury desired. The higher the pendulum, the more severe the injury. Once the pendulum is released, it strikes the back of a saline-filled cylinder that acts as a piston by then pushing saline through the craniotomy site causing a direct brain deformation injury. The pressure with which the fluid is injected causes the injury. The righting reflex time is used as an indication of injury severity.

The control used in these experiments are SHAM injured animals who have undergone the craniotomy and the same procedures as the injured animals with the exception of the fluid percussion injury itself. The term "ipsilateral" will be used when referring to the brain hemisphere that underwent the craniotomy in the lateral FPI procedure while "contralateral" refers to the opposite brain hemisphere.

Craniotomy. Male Sprague-Dawley rats (300–450 grams) were anesthetized (4% isoflurane) and prepared for moderate or sham parasagittal fluid percussion injury (FPI). Rectal temperatures were monitored using telethermometers (Yellow Spring Instrument Co., Yellow Springs, OH), and temperatures were maintained within a range of 37.5 ± 0.5 °C using an overhead lamp and a thermostatically controlled water blanket (Gaymar, Orchard Park, NY). Rats were placed in a stereotaxic apparatus, a midline incision of the skin was performed, and the skull was exposed. A craniotomy was performed using a 5mm diameter Michele trephine at 1 mm lateral (right) to the sagittal suture, midway between the lambda and bregma. The bone chip was removed, leaving the dura intact. A modified 20-gauge needle hub was secured in place over the exposed dura with superglue and cemented into place with hygienic dental acrylic.

Parasagittal Fluid Percussion Injury. TBI was administered by means of a FPI device (AmScien Instuments, Richmond, VA) consisting of a fluid-filled Plexiglass cylinder 25-inches-

long and 2.5 inches in outside diameter, with one end connected to a pressure transducer and the other end closed by a Plexiglass piston mounted on O rings. The animal's craniotomy hub site was directly connected to the transducer end of the injury device. The 3.6-kg pendulum of the device was lifted to a specified height to correspond to the intensity of injury desired, moderate injury level for these studies. The pendulum was released and struck the back of the sterile saline-filled cylinder causing a direct brain deformation injury. The fluid pressure pulse is triggered photoelectrically by the strike of the pendulum and was recorded using a FP-302 signal conditioner connected to a Windows 8 operating computer. The righting reflex time was recorded and further used as an indication of injury severity. At 2 days, 7 days, 1 month, or 3 months after TBI or sham injury, the rats were euthanized and brain tissue collected as described above.

Synaptosomal Isolation

Synaptosomes containing both pre- and post-synaptic components were isolated from frozen tissue that had been snap frozen on dry ice and transferred to -80°C. Left and right hippocampi were homogenized separately in SynPER (Thermo Scientific, Waltham, MA) with 1% protease (Sigma, St. Louis, MO) and phosphatase cocktail inhibitors (Thermo Scientific, Waltham, MA) on ice. Homogenate was centrifuged (Eppendorf, Mississauga, Canada) at 1,200 x g RCF for 10 minutes at 4°C. Supernatant was collected and centrifuged (Eppendorf, Mississauga, Canada) at 15,000 x g RCF for 20 minutes at 4°C. The supernatant was removed, and the pellet was resuspended in 48μL HEPES-buffered Krebs-like (HBK) buffer (143-mM NaCl, 4.7-mM KCl, 1.3-mM $MgSO_4$, 1.2-mM $CaCl_2$, 20-mM HEPES, 0.1-mM NaH_2PO_4, and 10-mM D-glucose, pH 7.4). The quality of the synaptosomes are routinely verified by Western blot and electron microscopy as previously reported[65].

Michael Woodson from the UTMB electron microscopy core used frozen, isolated synaptosomes to generate the electron microscopy images shown in Figure 7D.

Insulin Responsiveness

Insulin Stimulation of synaptosomes. After isolation of synaptosomes, insulin stimulations were performed as previously described[65–67]. In short, 100mM ATP stock was added for final concentration of 8mM to synaptosomes in HBK for both unstimulated and stimulated samples, and U-100 insulin was added for 200nM final insulin concentration to insulin-stimulated samples. Samples were vortexed and incubated for 15 minutes at 37°C. Synaptosomes were pelleted by centrifugation at 10,000 x g RCF for 10 minutes at 4°C. Pellets were resuspended in 1X RIPA (75-mM NaCl, 25- mM Na2PO4, 1-mM EDTA, 0.5% NP-40, and 0.5% TritonX-100) plus 1% protease (Sigma, St. Louis, MO) and phosphatase cocktail inhibitors (Thermo Scientific, Waltham, MA) to solubilize the proteins for Western blot and WES detection. Samples were then stored at -80°C.

WES analysis of Insulin Responsiveness. IR phosphorylation extent was analyzed using WES (Protein Simple, San Jose, CA) with specific antibodies against the phosphorylated form of the 1150/1151 tyrosine residue of the insulin receptor (Cell Signaling Cat. #3024L). The phosphorylated form was normalized against β-tubulin (Cell Signaling Cat. #2146S). Another WES was run for the total amount of IR (Cell Signaling Cat. #3025S) which was normalized to β-tubulin as well. The ratio of normalized phosphorylated-IR over normalized total IR was used to assess the extent of insulin responsiveness.

Western Blot Analysis for SOCS3

The bicinchoninic acid (BCA) assay method was used for protein estimation to prepare samples of equal protein concentration. Samples were prepared in 2-mercaptoethanol (2-ME) and boiled prior to loading. Thirty micrograms of protein were loaded with appropriate marker on 10%

sodium dodecyl sulfate polyacrylamide gel electrophoresis (SDS-PAGE) gels followed by transfer to Amersham Protran nitrocellulose transfer membrane (GE Healthcare-Life Sciences) for 1 hour at 100V. The membrane was blocked using Odyssey blocking buffer (LI-COR, Lincoln, Nebraska) for 1 hour at room temperature. Primary antibodies were diluted 1:1000 in 1X TBST and incubated with the membrane at 4°C overnight for SOCS3 (Cell Signaling Cat. #2923S) and 1 hour at room temperature for β-tubulin (Cell Signaling Cat. #2146S). The membrane was washed twice with 1X TBST for 15 minutes each and incubated with LI-COR secondary antibodies diluted at 1:10,000 in 1X TBST with 3% non-fat dry milk for 1 hour at room temperature. The membrane was again washed twice with 1X TBST for 15 minutes each.

Western blots were imaged using LI-COR Odyssey infrared imaging system (LI-COR, Lincoln, Nebraska), application software version 3.0.30. The density of each immunoreactive band was measured using Image J software.

Aβ-binding

Aβ oligomer preparation. Human Aβ1–42 peptide was purchased from Department of Biophysics and Biochemistry, Harvard University, MA. Human Aβ oligomers are routinely prepared in our lab [68] from lyophilized synthetic Aβ aliquots of 0.3mg. 200µL of 1,1,1,3,3,3-Hexafluro-2-propanol (HFP) was used to dissolve the lyophilized aliquots. 700µL of DDI water was then added, and a cap with four holes was placed on the tube. The sample was magnetically stirred under a fume hood for 48 hours. The Aβ oligomers were aliquoted, frozen at -80°C, and used within 3 months. For the flow cytometry analysis of Aβ oligomer-binding to synaptosomes, Aβ oligomers spiked with Flour 647 tagged Aβ (AnaSpec Inc., Fremont, CA) were utilized. These Aβ oligomers were prepared by adding 7µL of the tagged Aβ to the HFP-Aβ mixture described above, prior to the addition of water. The quality of the oligomeric preparations was routinely

checked by Western blot and dot blot analysis using 6E10 and A-11 antibodies (Aβ oligomer specific).

Aβ oligomer binding challenge. Oligomeric Aβ to be employed in the same experiment was always used from aliquots of the same batch of Aβ. Hippocampal synaptosomes were treated with Aβ oligomers for an *ex vivo* binding challenge and evaluated using flow cytometry as previously performed in our lab[69]. An equal number of isolated synaptosomes per animal determined by flow cytometry were pooled for each experimental group. For each group, the pooled samples were then aliquoted into 10 separate tubes containing 10 million synaptosomes each. This was repeated 3 times for 3 separate curves. Each sample was incubated with Aβ oligomers tagged with HyLite Fluor 647 for the desired μM concentration, ranging from 0 μM to 20 μM, for 1 hour at room temp. Synaptosomes were then centrifuged at 15,000 x g RCF for 10 minutes at 4°C, washed 3 times with HBK buffer, and resuspended in PBS. Data was acquired by a Guava EasyCyte flow cytometer (EMD Millipore, Burlington, MA) and analyzed using Incyte software (EMD Millipore).

Tau-binding

Tau-oligomer preparation. Prepared recombinant tau oligomers were graciously given to us by Dr. Rakez Kayed's laboratory. The tau oligomers were produced as previously described [70]. Briefly, full-length human recombinant tau was expressed, purified, and aliquoted into a monomeric tau stock solution of 1mg/mL in 1XPBS buffer at pH 7.4. Aβ42 oligomers seeds were added to a 0.3 mg/ml tau solution in 1XPBS and incubated on an orbital shaker for 1 hour at room temperature. The tau oligomers produced were purified by FPLC and used as seeds in a fresh batch of tau monomers. After three rounds of seeding with purified tau oligomers, detection of the original Aβ seeds was eliminated due to sufficient dilution. Each batch of oligomers is tested using

dot blot with T22 (a tau oligomer-specific antibody), Western blot analysis, and atomic force microscopy (AFM) to verify the quality of the tau oligomer preparation.

Ex vivo Tau-oligomer binding. Synaptosomes were treated with tau oligomers for an ex vivo binding challenge and evaluated using ELISA as previously performed in our lab [71]. Hippocampal synaptosomes from each animal were challenged and evaluated independently. Using flow cytometry, 10 million synaptosomes from each animal were aliquoted and challenged with 2 µM of tau oligomers for 1 hour at room temperature. The samples were then centrifuged and washed with HBK buffer 3 times to thoroughly remove any unbound tau oligomers. Synapse number was acquired using flow cytometry once again, and an equal amount of synaptosomes per sample were analyzed by tau5 ELISA.

ELISA Analysis of Tau. Total tau levels were measured by ELISA analysis using the total tau antibody tau5 (Biolegend Cat. # 806401). Samples were incubated on the ELISA plate at 4 °C overnight with the coating buffer 0.1 M sodium bicarbonate (pH 9.6). Samples were discarded and each well was washed with Tris-buffered saline with low Tween 20 (0.01%) (TBS-low T) followed by blocking with 10% nonfat milk for 2 hours. After a second wash, the primary tau5 antibody (1:1000 in 5% nonfat milk in TBS-low T; Thermo Scientific) was incubated in each well for 1 hour at room temperature. After a third wash, the plates were incubated for 1 hour at room temperature with horseradish peroxidase-conjugated anti-rabbit IgG secondary antibody (1:10,000 in 5% nonfat milk in TBS-low T; Promega). Following the fourth wash, 3,3,5,5-tetramethylbenzidine (TMB-1 component substrate; Sigma-Aldrich) was added to each well. After 30 min of incubation in the dark, 1 M HCl was added to stop the reaction, and the plate was read at 450 nm for tau detection and quantification.

Electrophysiology

Animals were euthanized with deep isoflurane anesthesia, decapitated by guillotine, and brains were harvested and sliced using Compresstome VF-300 (Precisionary Instruments, Greenville, NC) in NMDG-aCSF (93 mM NMDG, 2.5 mM KCl, 1.2 mM NaH2PO4, 30 mM NaHCO3, 20 mM HEPES, 25 mM glucose, 5 M sodium ascorbate, 2 mM thiourea, 3 mM sodium pyruvate, 10 mM MagSO4·7H20, 0.5 mM CaCl2·2H2O, and 12 mM N-acetyl L-Cysteine) to obtain 450 μm transverse brain sections. Slices were allowed to recover for 10 minutes in NMDG-aCSF at 35°C. Slices were then maintained at room temperature in a modified HEPES holding aCSF solution (92 mM NaCl, 2.5 mM KCl, 1.2 NaH2PO4, 30 mM NaHCO3, 20 mM HEPES, 25 mM Glucose, 5 mM sodium ascorbate, 2 mM thiourea, 3 mM sodium pyruvate, 2 mM MgSO4 7H20, 2 CaCl2 2H20, 12 N-Acetyl L-Cysteine). Slices were recorded in standard recording aCSF (124 mM NaCl, 2.5 mM KCl, 1.2 mM NaH2PO4, 24 mM NaHCO3, 5 mM HEPES, 12.5 mM glucose, 2 mM MgSO4·7H20 and 2 mM CaCl2·2H20). All solutions were aerated using 95% O2 with 5% CO2. For oligomer challenges, the slices were incubated for 1 hour at room temperature prior to recording with 200nM Aβ oligomers, 50nM tau oligomers, and/or 200nM insulin. For slices treated with insulin, 200nM insulin was also present in the aCSF recording solution. Using a horizontal P-97 Flaming/Brown micropipette puller (Sutter Instruments, Novato, CA), borosilicate glass capillaries were used to pull electrodes and filled with nACSF to get a resistance of 1–2 MΩ. Evoked field excitatory post-synaptic potentials (fEPSPs) recordings were performed by stimulating the Schaffer collateral pathway using a stimulating electrode of 22 kΩ resistance placed in the CA3 region and recording in the CA1 region. LTP was induced using an HFS protocol (3 x 100 Hz, 20 seconds) as previously described [72]. Recordings were digitized with Digidata 1550B (Molecular Devices, Sunnyvale, CA), collected using an Axon MultiClamp 700B differential amplifier (Molecular Devices), and analyzed using Clampex 10.6 software (Molecular

Devices). Current stimulation was delivered through a digital stimulus isolation amplifier (A.M.P.I, ISRAEL) and set to elicit an fEPSP approximately 30% of maximum for synaptic potentiation experiments using platinum-iridium tipped concentric bipolar electrodes (FHC Inc., Bowdoin, ME). Baseline recordings were obtained by delivering single pulse stimulations at 20 second intervals. All data are represented as a percentage change from the initial average baseline fEPSP slope obtained for the 10 minutes prior to HFS.

Insulin's Effect on Properties of Hippocampal Slices

Naïve, male Sprague-Dawley rats were euthanized with deep isoflurane anesthesia, decapitated by guillotine, and brains were harvested and sliced as performed for the electrophysiology experiments. Slices were then maintained at room temperature in a modified HEPES holding aCSF solution and aerated using 95% O_2 with 5% CO_2.

Effect on Aβ binding.　　　　Hippocampal brain slices were treated with Aβ oligomers ± insulin, synaptosomes isolated, and binding evaluated using flow cytometry. Slices were challenged with 2.5µM Aβ-oligomers tagged with HyLite Fluor 647 diluted in HEPES holding aCSF solution with or without 200nM insulin to mimic the insulin stimulation used for the electrophysiology paradigm. A higher concentration of Aβ-oligomers was used for these experiments than for the electrophysiology (2.5µM rather than 200nM) because the flow cytometry detection method used here cannot detect 200nM Aβ binding parameters. Each slice was incubated in 0.5mL total solution in a 48 well cell/tissue culture plate (Costar, Corning, NY) for 1 hour in the dark in a 37°C tissue incubator maintained with 95% O_2 with 5% CO_2. Slices were transferred to 1.5mL tubes and washed with HEPES-aCSF to remove any unbound oligomers. Synaptosomes were isolated using SynPER as described above and resuspended in PBS. Data was acquired by a Guava EasyCyte

flow cytometer (EMD Millipore, Burlington, MA) and analyzed using Incyte software (EMD Millipore).

Effect on mitochondria. Hippocampal brain slices were treated with insulin, synaptosomes isolated, mitochondria labeled, and flow cytometry used to evaluate mitochondria. Slices were treated with either 200nM or 2.5µM of insulin diluted in HEPES holding aCSF solution for 1 hour in a 37°C tissue incubator maintained with 95% O2 with 5% CO2. Slices were transferred to 1.5mL tubes and washed with HEPES-aCSF, and synaptosomes were isolated using SynPER as described above. Synaptosomes were then treated with Mitotracker green FM (Invitrogen, Carlsbad, CA) and MitoSense Red (1,1′,3,3,3′,3′- Hexamethylindodicarbocyanine iodide) (EMD Millipore, Burlington, MA) for 15 minutes at 37 °C. MitoTracker is a fluorescent dye that diffuses across the mitochondrial membrane and reacts with thiol groups of specific mitochondrial proteins[73]. The fluorescent dye MitoSense correlates with mitochondria membrane potential[74]. The synaptosomes were washed twice with HBK buffer and then resuspended in PBS. Fluorescent emittance was acquired by a Guava EasyCyte flow cytometer (EMD Millipore, Burlington, MA) and analyzed using Incyte software (EMD Millipore).

Statistical Analysis

Data is represented as mean ± SEM except for electrophysiology data represented as mean ± SD. All data were statistically analyzed using Graphpad Prism6. Unpaired t-tests were used to determine statistical significance between sham and TBI animals for each time point individually for the insulin stimulations and oligomer binding experiments. For the electrophysiology experiments, a one-way ANOVA with Bonferroni's post hoc test was used to determine statistical significance between the LTP of each condition.

B. Results

<p align="center">I. **Investigating synaptic insulin resistance after FPI**</p>

Development of *ex vivo* insulin stimulation method:

In order to investigate and assess insulin responsiveness, I had to develop a method whereby I would be able to detect phosphorylation of the insulin receptor directly, rather than probing for downstream elements. Additionally, I wanted to isolate responses of neurons at the synapse to avoid picking up IR activation at the cell body or in other cell types such as glia. Therefore, I developed an *ex vivo* insulin stimulation method on isolated synaptosomes, details of which can be found in my published method paper in Journal of Neuroscience Methods[65].

To accomplish this detection method, I isolate functional synaptosomes containing both pre and post-synaptic elements (Figure 7A) from fresh or frozen tissue by fractionation (either using a Percoll sucrose gradient or using synPER reagent (Thermo Scientific)) and expose them to insulin in the presence of ATP to detect insulin receptor phosphorylation using either Western blot or WES analysis.

Isolation and confirmation of synaptosomes and IR responsiveness.

Upon initially developing the method, I used electron microscopy to visually confirm synaptosomal isolation (Figure 7D). I additionally confirmed the isolation of the synaptosomes by checking for enrichment of post-synaptic density marker PSD-95 in the synaptosomal fraction versus total homogenate using Western blot analysis (Figure 7B). I saw an enrichment of this marker in the synaptosomal protein fraction indicating that the fractionation procedure was successful. Moreover, I demonstrated a reliable phosphorylation of the insulin receptor (IR) via Western blot analysis using this method (Figure 7C).
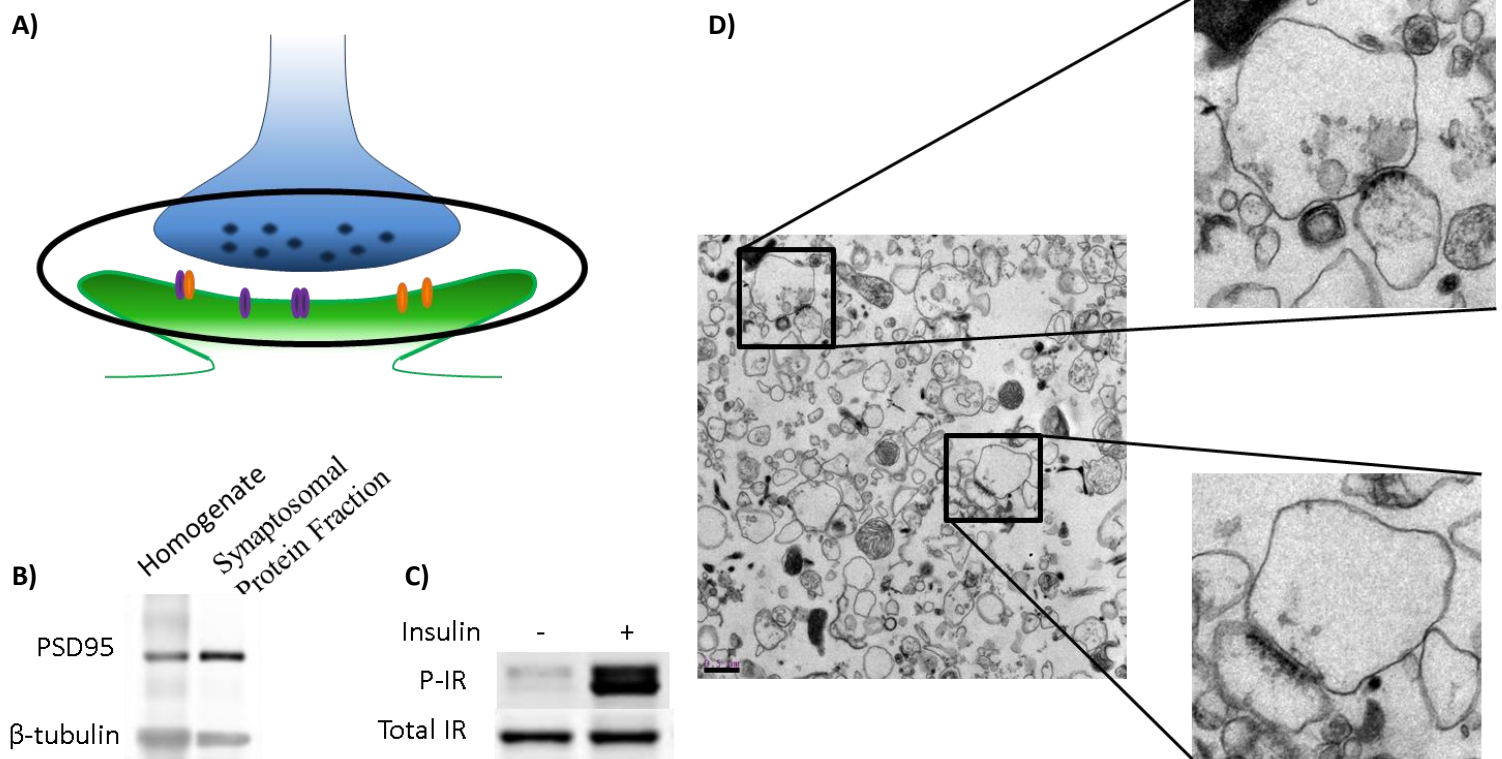
Figure 7: Synaptosomal characterization and confirmation of insulin stimulation. A) A schematic showing the pre- and post-synaptic areas retained in the synaptosomal isolation. B) Representative Western blot detecting enrichment of the post-synaptic marker PSD95 in synaptosomal fraction versus total homogenate, indicating successful synaptosomal isolation. C) Representative Western blot detecting insulin-stimulated IR phosphorylation in synaptosomes isolated from frozen rat brain and stimulated with 0.333 units/mL of insulin for 15 min at 37°C with 8mM ATP. D) Representative transmission electron microscopy image (3,000 x) of synaptosomal protein fraction. Scale bar represents 0.5µm. Blow-out insert images illustrate examples of synaptosomes characterized by the presence of the post-synaptic density area (arrows). [Modified from Figure 1 and Supplemental Figure 2 from Franklin et al., 2016]

Optimization of ex vivo insulin stimulation conditions.

After confirming synaptosomal isolation as well as confirmation that this *ex vivo* insulin stimulation allows for detection of the insulin receptor directly, I optimized this technique with ATP dosage curves, insulin dosage curves, and insulin time course responses. From the data investigating insulin-stimulated IR phosphorylation of synaptosomes isolated from frozen rat brain tissue that were stimulated with 1.67 units/mL of insulin for 15 min at 37 °C in the presence of increasing concentrations of ATP (0–6 mM ATP) in the incubation buffer, I saw no plateau in

insulin receptor activity in this concentration range as determined by Western blot (Figure 8A). Since the ATP concentration inside the cell is between 0 and 10 mM, I decided to use an ATP concentration of 8mM for all future experiments. Using synaptosomes from frozen mouse brain and stimulating with increasing concentrations of insulin for 15 min at 37 °C in the presence of 8 mM ATP, I saw a plateaued response beginning at 0.154units/mL of insulin (Figure 8B). An insulin-receptor activation curve of synaptosomes exposed to 0.333 units/mL of insulin for varying amounts of time from 0 to 1 h at 37°C with 8 mM ATP was performed and analyzed by western blot. I found maximal IR phosphorylation 10 to 15 minutes after addition of insulin (Figure 8C) and thus used 15-minute incubations for the remaining experiments.

Furthermore, I looked at other factors that may influence the ability of the IR to activate including post-mortem intervals (PMI) (Figure 8D). I looked at PMIs that modeled the conditions that would normally occur for collection of autopsy brain human specimens (PMI of 8 hours, 12 hours, and 21 hours). To accomplish this, I assessed insulin-stimulated phosphorylation of the IR in synaptosomes isolated from brain tissue collected from mice at varying times after sacrifice. Mice were sacrificed by CO_2 asphyxiation followed by cervical dislocation and left at room temperature for 1 hour prior to being placed at 4°C for the remainder of the specified PMI times. Afterwards, brains were collected, snap frozen, and stored at -80°C. Synaptosomes were isolated from the frozen mouse brains and stimulated with 0.333 units/mL of insulin for 15 min at 37°C with 8mM ATP. I found no significant differences in the ratio of P- IR/IR in the various PMI samples versus control where the brain was immediately collected and placed at −80°C upon sacrifice.
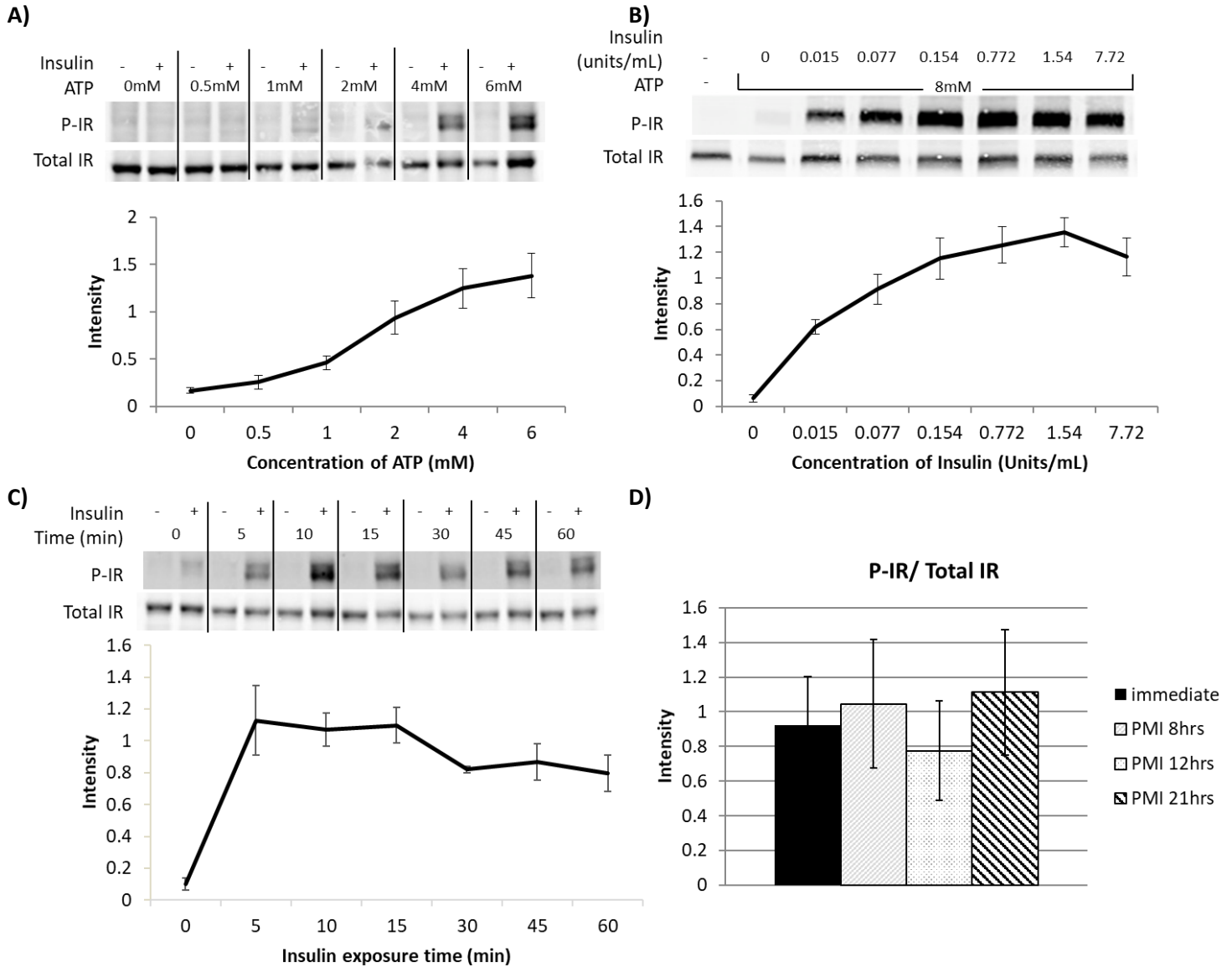
Figure 8: Optimization of ex vivo insulin stimulation method. A) Representative Western blot of insulin-stimulated IR phosphorylation in the presence of increasing concentrations of ATP in the incubation buffer and quantification of the ratio p-IR/Total IR expressed as average ±SEM from 3 independent experiments. B) Representative Western blot showing IR phosphorylation in response to increasing concentrations of insulin and quantification of the ratio p-IR/Total IR expressed as average ±SEM from 3 independent experiments. C) Representative Western blot showing IR phosphorylation at different time points after insulin addition and quantification of the ratio p-IR/Total IR expressed as average ±SEM from 3 independent experiments. D) Quantification of Western blot's immunoreactivity from insulin-stimulated phosphorylation of the IR in synaptosomes isolated from brain tissue collected from mice at varying post-mortem intervals. [Modified from Figure 2 and Figure 4 from Franklin et al., 2016]

Comparison of ex vivo and in vivo synaptosomal insulin response.

After optimization of the method, I wanted to verify that the *ex vivo* insulin stimulation protocol yields results consistent with *in vivo* physiology by using a transgenic mouse model of metabolic syndrome and systemic insulin resistance, AtENPP1-Tg. This mouse model has previously been shown to present with marked synaptic insulin resistance when assessing downstream insulin signaling elements (AKT and GSK3β) after an intraperitoneal (IP) insulin injection (*in* vivo insulin stimulation), contrary to the response seen in wild-type (WT) mice [63] (Figure 9A).

Thus, to confirm that the *ex vivo* results were consistent with the *in vivo* situation, I isolated synaptosomes from both the WT and AtENPP1-Tg mice, performed this *ex vivo* insulin stimulation protocol, and observed IR phosphorylation/activation to a lesser extent in the transgenic animals compared to controls (Figure 9B). This data clearly shows that this *ex vivo* stimulation correlates and represents the physiology *in vivo* due to detection of a decreased response of the insulin receptor in an animal model of known insulin resistance.
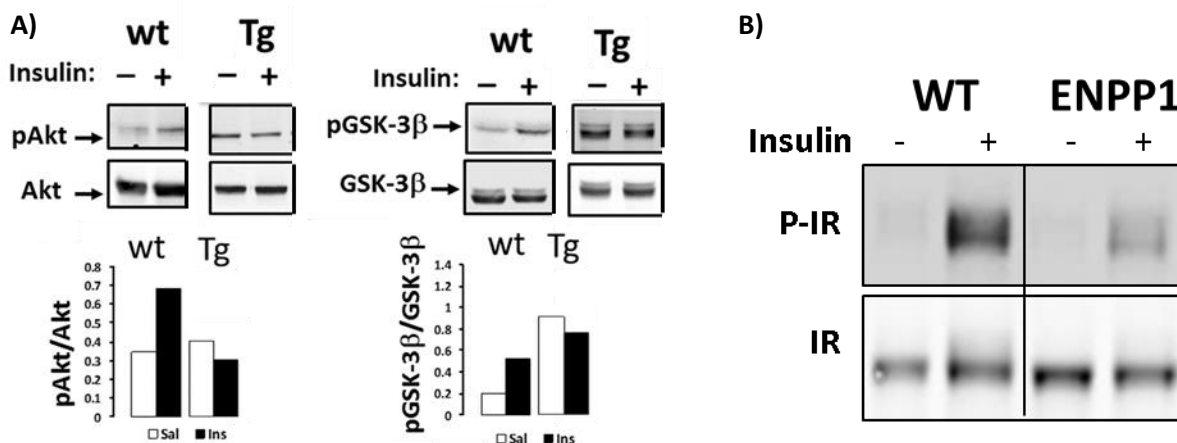
Figure 9: Comparison of in vivo and ex vivo synaptosomal insulin response. A) In vivo insulin response in the hippocampus of AtENPP1-Tg mice showing blunted post-receptor response to systemic insulin elevation (IP insulin injection) compared to their WT littermates [Modified from Figure 1S Sallam et al., 2015]. B) Representative Western blot detecting insulin-driven phosphorylated IR in isolated hippocampal synaptosomes from AtENPP1-Tg and WT mice using the *ex vivo* insulin stimulation technique [Adapted from Figure 5 Franklin et al., 2016].

Evaluate synaptosomal insulin responsiveness after TBI:

Now with an established technique in place to evaluate synaptic insulin receptor responsiveness, I tested the hypothesis that TBI alters insulin responsiveness at the synapse after FPI in rats. I performed lateral FPI to induce TBI, collected and dissected the brain, and performed *ex vivo* insulin stimulations and WES analyses on isolated synaptosomes of frozen brain tissue prepared from the hippocampi of both the ipsilateral-hemisphere (side of injury) and contralateral-hemisphere (opposite to the lateral injury). I evaluated multiple time-points after injury (2 days post injury (DPI), 7 DPI, 1-month post injury (MPI), and 3 MPI).

In the ipsilateral hippocampus, I found a significant decrease in synaptic insulin responsiveness by 7 DPI (Figure 10B) that was further decreased by 3 MPI. Moreover, I observed a significantly decreased level of IR at the synapse at 7DPI, as compared to sham-injured animals (Figure 10C). However, this decrease in IR level cannot account for the decreased insulin response at this time-point after injury. At 1 MPI, the synaptic IR level was normalized back to the level of sham-injured animals, and there was a further significant increase in IR level at the synapse at 3 MPI which could be indicative of an attempted compensatory mechanism. I also found a significant increase in basal (unstimulated) level of IR phosphorylation at 2 DPI (data not shown). Whereas at both 7 DPI and 3 MPI, the basal level of IR phosphorylation was significantly decreased (data not shown).
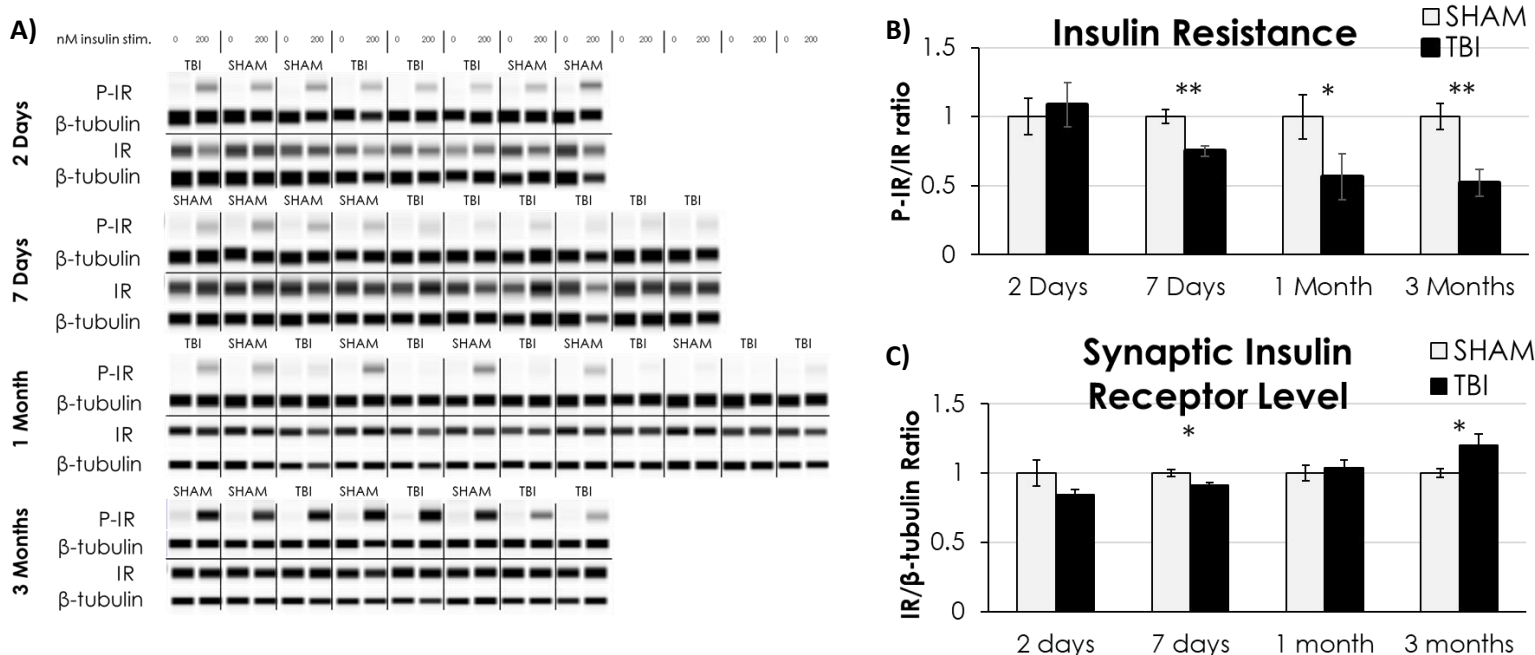
Figure 10: Insulin Responsiveness in Ipsilateral Hippocampus. A) Representative WES analysis of insulin stimulated and unstimulated isolated synaptosomes from 2 DPI (n =4 for both sham and TBI), 7 DPI (n= 4 sham, n=6 TBI), 1 MPI (n= 5 sham, n=7 TBI), and 3 MPI (n= 4 for both sham and TBI) animals. Quantitative graph of WES analysis showing B) the ratio of P-IR/β-tubulin to IR/β-tubulin demonstrating that synaptosomal insulin responsiveness is chronically decreased after TBI and C) IR/β-tubulin showing the changes in insulin receptor level at the synapse. Statistical significance was determined by unpaired t-test analysis. Error bars represent standard error. *p < 0.05; **p < 0.01.

In the contralateral hippocampus, there was a significant decrease in IR response to insulin at 7 DPI and 3 MPI (Figure 11B). Interestingly though, unlike the ipsilateral hippocampus, I found no difference in synaptic IR level in the contralateral hippocampus at any of the time points studied (Figure 11C). There was, however, a significantly decreased basal level of IR phosphorylation in TBI animals at 7 DPI that then returned to normal levels by 1 MPI (data not shown).
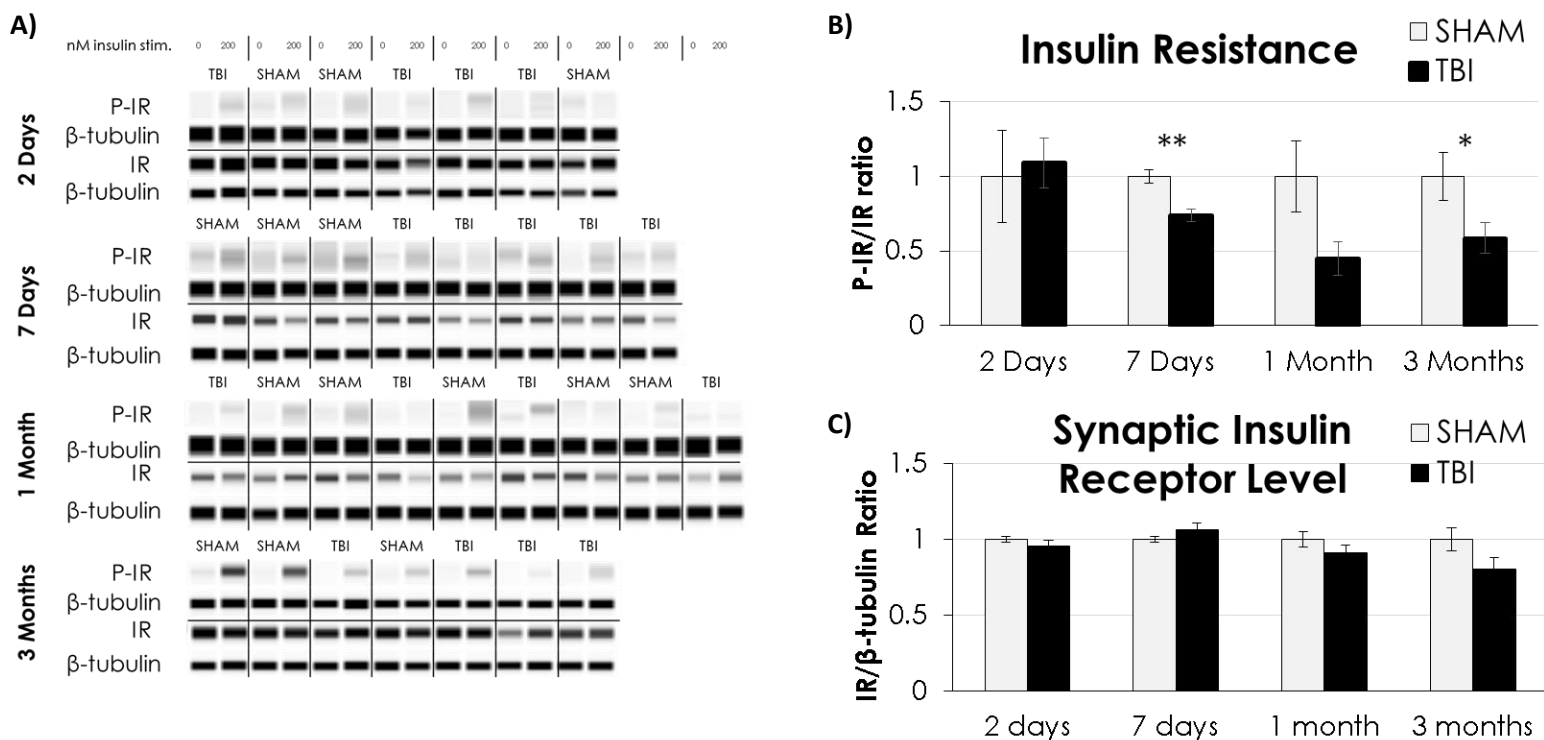
Figure 11: Insulin Responsiveness in Contralateral Hippocampus. A) Representative WES analysi of insulin stimulated and unstimulated isolated synaptosomes from 2 DPI (n =3 sham, n=4 TBI), 7 DPI (n= 3 sham, n=5 TBI), 1 MPI (n= 5 sham, n=4 TBI), and 3 MPI (n= 3 sham, n= 4 TBI) animals. Quantitative graph of WES analysis showing B) the ratio of P-IR/β-tubulin to IR/β-tubulin demonstrating that synaptosomal insulin responsiveness is chronically decreased after TBI and C) IR/β-tubulin showing that the insulin receptor level at the synapse is unchanged. Statistical significance was determined by unpaired t-test analysis. Error bars represent standard error. $*p < 0.05$; $**p < 0.01$.

In summary, I found a significant decrease in the synaptic insulin receptor's response to insulin at 7 DPI, 1 MPI, and 3 MPI but not at 2 DPI. These data indicate that there are chronic deficits in synaptic insulin responsiveness in both the ipsilateral and contralateral hippocampi after lateral FPI.

Assess possible mechanistic driver of synaptic insulin resistance:

I then decided to turn my attention to a possible mechanistic driver of this chronic synaptic insulin resistance that I found. Thus, I thought to look for an increased protein level of an insulin receptor inhibitor that could directly bind to the insulin receptor. I first decided to try and look at

ENPP1, a pyrophosphatase that not only degrades ATP but can directly bind to the insulin receptor to remove and prevent phosphorylation. After multiple attempts in a variety of samples, I determined that I could not see a sufficient amount of ENPP1 in any hippocampal rodent brain samples (homogenate, cytosol, synaptosomes ± insulin) (data not shown) which suggests that either ENPP1 is not at a detectable protein level in the brain or that the antibody for this protein is not specific enough to prove to be a viable method of detection and analysis.

I then performed a more in-depth literature search for inhibitor candidates, and, with the help of employing the brain atlas protein database, I determined an alternative protein to investigate as the insulin receptor inhibitor. I decided to look for an upregulation of SOCS3. SOCS3 is a protein of the suppressor of cytokine signaling (SOCS) family that acts as negative regulators of cytokine and growth factor signaling. SOCS3 expression can be induced by IL6 as well as IL10 and has previously been shown to negatively regulate insulin signaling[75]. I analyzed the level of this protein in synaptic fractions from hippocampi of both brain hemispheres in sham and TBI animals at all of my time points (2 DPI, 7 DPI, 1 MPI, and 3 MPI) using Western blot analysis (Figure 12).

In the ipsilateral hippocampus, I found a significantly increased level of SOCS3 at the synapse in TBI animals versus sham animals at 2 DPI, 7 DPI, and 1 MPI as well as a trend of a remaining but not significant increase at 3 MPI (Figure 12A/C). Since this occurs prior to insulin resistance being found at the synapse at 7 DPI, this could be a driving factor in initiating the dysregulation and insulin resistance. In the contralateral hemisphere, however, I did not find altered levels of SOCS3 at the synapse at any of the time points (Figure 12B/D). While I still found synaptic insulin resistance beginning at 7 DPI in this hemisphere too, it is possible that the two hemispheres have resulting insulin resistance from different mechanisms.
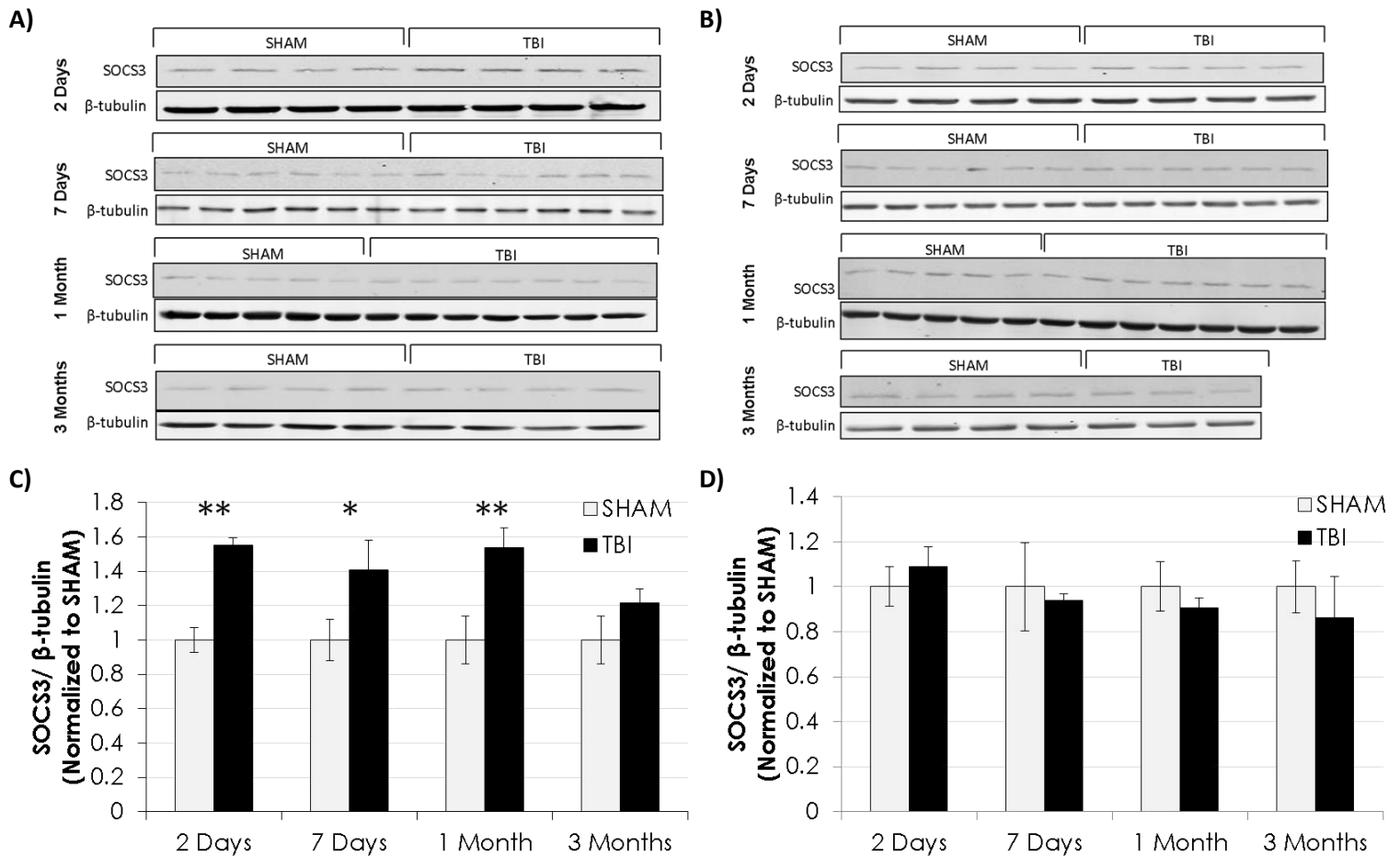
Figure 12: SOCS3 Expression in the Ipsilateral and Contralateral Hippocampi. Western blots of isolated synaptosomes from 2 DPI (n = 4 for both sham and TBI), 7 DPI (n= 6 for both sham and TBI), 1 MPI (n= 5 sham, n=7 TBI), and 3 MPI (n= 4 sham, n= 4 TBI ipsi and n=3 TBI contra) animals isolated from the A) ipsilateral hippocampus and B) contralateral hippocampus. Quantitative graphs of the Western blot analysis showing SOCS3 normalized to β-tubulin for the C) ipsilateral hippocampus and D) contralateral hippocampus. Statistical significance was determined by unpaired t-test analysis. *p < 0.05; **p < 0.01.

II. Evaluating synaptic vulnerability to the effects of Aβ and tau after TBI

To investigate whether the chronically decreased synaptic insulin responsiveness may lead to increased synaptic sensitivity to AD pathology, I decided to evaluate synaptic vulnerability to these proteinaceous species in two ways; binding susceptibility and functional vulnerability.

Quantify synaptosomal Aβ binding after TBI:

I tested the hypothesis that synaptic vulnerability to Aβ binding is increased after TBI by utilizing an *ex vivo* Aβ binding protocol with flow cytometry analysis to generate a binding concentration curve for Aβ. After learning flow cytometry and optimizing this experiment, I used isolated synaptosomes and performed an Aβ binding curve using 10 different concentrations of Aβ oligomers labeled with Flour 647 (from 0 µM to 20 µM) with 3 replicates of pooled samples of 1 and 3 MPI animals from the ipsilateral (Figure 13B/C) and contralateral hippocampi (Figure 13D/E). To exclude non-synaptosomal particles in our analysis and eliminate any nonspecific Aβ oligomer-binding, I size-gated for synaptosomes with parameters set to include particle sizes from 1–5 µm. Data were transformed for Scatchard plot analysis to estimate the maximum binding capacity (B_{max}) and affinity (K_d) of Aβ binding. I did not find increases in Aβ binding (neither in V_{max} nor in K_d) in hippocampal synaptosomes from TBI versus sham animals at either the 1 month or 3 months post-injury time points. These results suggest that despite onset of insulin resistance, synapses are not more susceptible to Aβ oligomer binding at these intermediate and chronic time points.
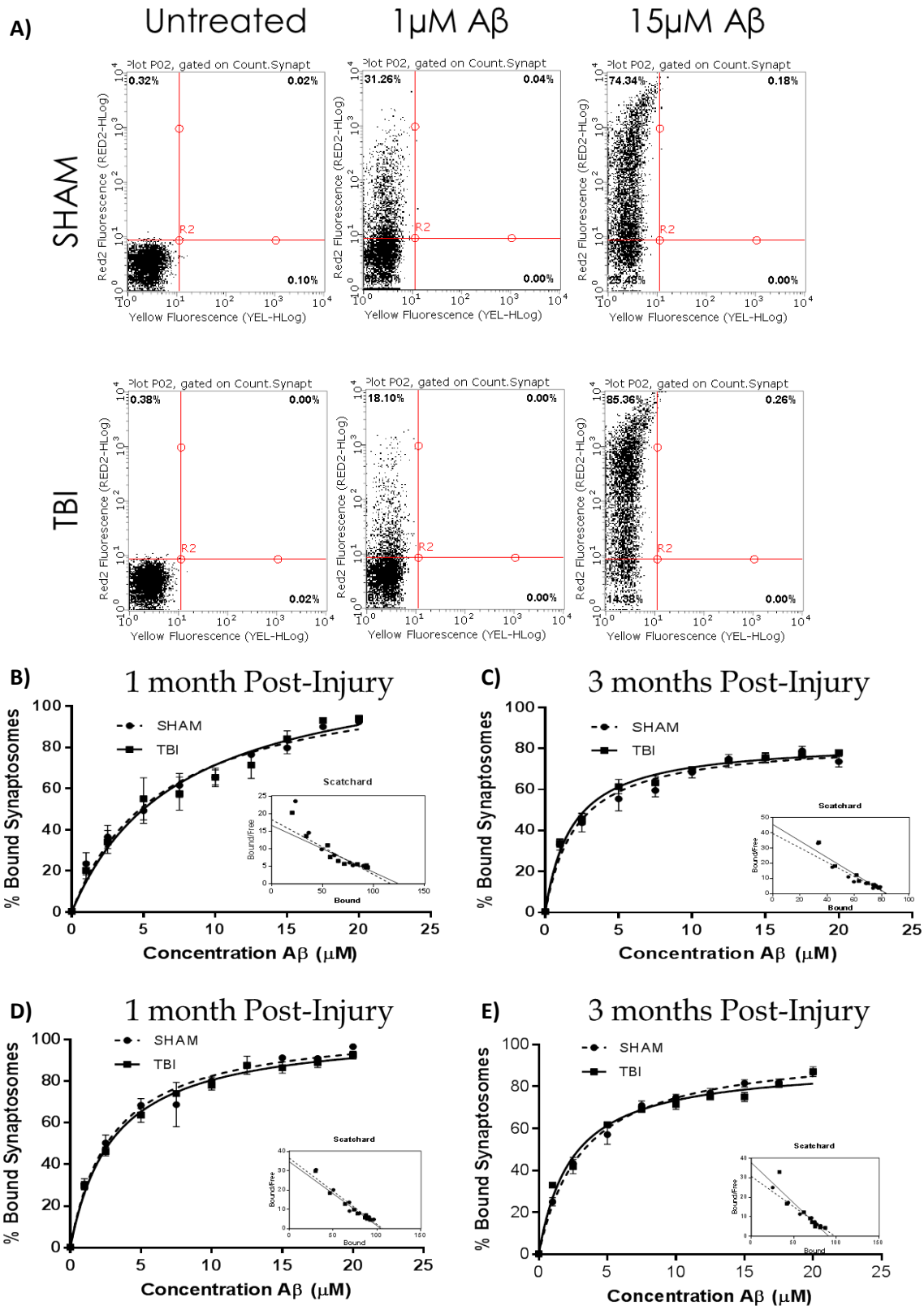
Figure 13: Amyloid-beta Oligomer *Ex Vivo* Binding Curves in the Ipsilateral and Contralateral Hippocampi. A) Representative flow cytometry analysis of pooled synaptosomes isolated from 1 MPI sham and TBI animals challenged with increasing concentrations of Aβ oligomers tagged with HyLite Fluor 647. Michaelis-Menton graphs with Scatchard plot transformation from three separate binding curve analysis showing the percent of synaptosomes with bound Aβ oligomers determined by flow cytometry analysis in the ipsilateral hippocampus at B) 1 month post-injury (n= 5 sham, n= 7 TBI) and C) 3 months post-injury (n= 4 for both sham and TBI) and in the contralateral hippocampus at D) 1 month post-injury (n= 5 sham, n= 7 TBI) and E) 3 months post-injury (n= 4 sham, n=3 TBI).

<u>Quantify synaptosomal tau binding after TBI:</u>

To complement the Aβ binding data at the intermediate and chronic time-points after TBI, my next goal was to determine tau binding in isolated hippocampal synaptosomes at these same time-points.

Therefore, to assess tau binding at the synapse, I performed an *ex vivo* binding experiment using a single concentration of tau on isolated hippocampal synapses and quantified the binding with an ELISA. I first optimized conditions for both the tau oligomer challenge as well as for the tau-5 ELISA on isolated rat synaptosomes. Tau-5 antibody showed high background from endogenous rat tau and thus took several experiments to optimize concentration/ incubation time of tau as well as sample concentration to load for the ELISA.

After optimization, to determine whether the chronically decreased synaptic insulin responsiveness would affect synaptic vulnerability to tau oligomers, I performed an *ex vivo* tau binding on hippocampal synaptosomes isolated from both sham and TBI animals at 1 month and 3 months post-injury using ten million synaptosomes from each animal and exposing them to 2μM of tau oligomers for 1 hour, as described in the Materials and Methods section. After washing synaptosomes to remove unbound oligomers, flow cytometry was used to ensure an equal number of synaptosomes were loaded per well for ELISA analysis. Tau-5 antibody was used to quantify the amount of tau bound to synaptosomes. I found that both ipsilateral (Figure 14A/B) and contralateral (Figure 14C/D) hippocampal synaptosomes from TBI animals at both time points bound similar levels of exogenously added tau oligomers as compared to sham animals. These data suggest that, similar to what I found for Aβ-oligomer binding, synapses are not more susceptible to tau oligomer binding at the late time points of 1 month or 3 months after TBI.
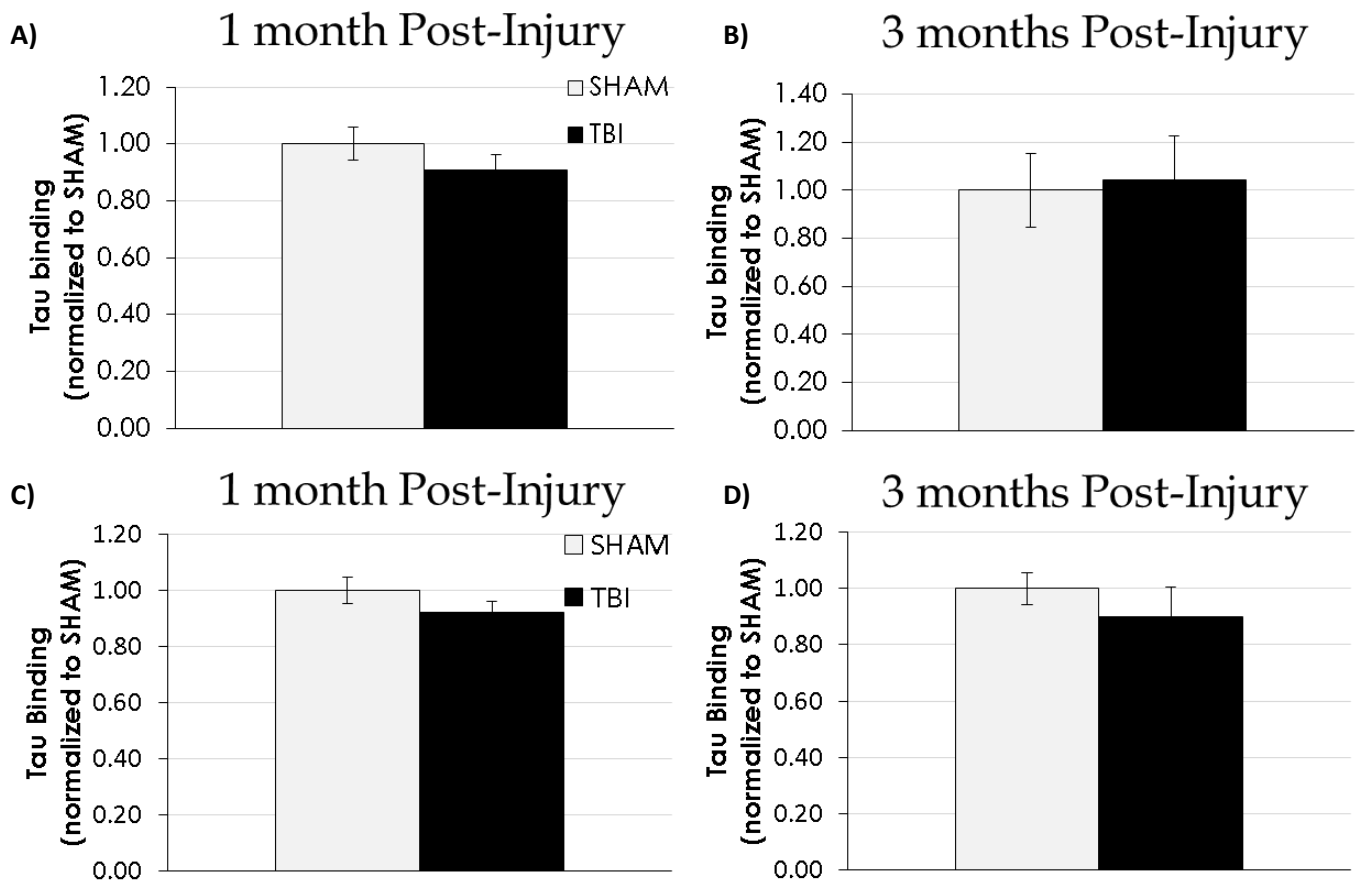
Figure 14: Ex Vivo Tau Oligomer Binding in the Ipsilateral and Contralateral Hippocampi.
Quantification of 2μM tau-oligomer *ex vivo* binding on isolated synaptosomes determined by tau-5 ELISA analysis in the ipsilateral hippocampus at A) 1 MPI (n= 5 sham, n= 7 TBI) and B) 3 MPI (n= 4 for both sham and TBI) and in the contralateral hippocampus at C) 1 MPI (n= 5 sham, n= 7 TBI) and D) 3 MPI (n= 4 sham, n= 3 TBI). Error bars represent standard error.

Electrophysiology Assessment:

While I did not observe any increases in hippocampal synaptic vulnerability to the binding of Aβ or tau oligomers in TBI animals, I wanted to test the hypothesis that there is an increase in functional vulnerability of synapses to AD pathology after TBI. Therefore, I decided to use electrophysiology to determine if there are functional disturbances that are commonly observed in both Aβ and tau oligomer-bound synapses, i.e. LTP inhibition. I sought to additionally evaluate

whether an application of insulin in coordination with the presence of the oligomers can block the oligomer-induced LTP suppression.

Hippocampal slices of the ipsilateral and contralateral hemispheres prepared from sham and TBI animals at both the 1 MPI and 3MPI time points were evaluated for LTP impairment after a treatment challenge with 200nM of Aβ oligomers (Figure 16 and Figure 18), 50nM of tau oligomers (Figure 17 and Figure 19), and/or 200nM insulin for 1 hour prior to recording. The electrophysiological assessment recorded from the Schaffer collateral pathway in untreated and oligomer-treated slices was performed using standard recording aCSF. When insulin treatment was used, slices were recorded using standard recording aCSF containing 200nM insulin.
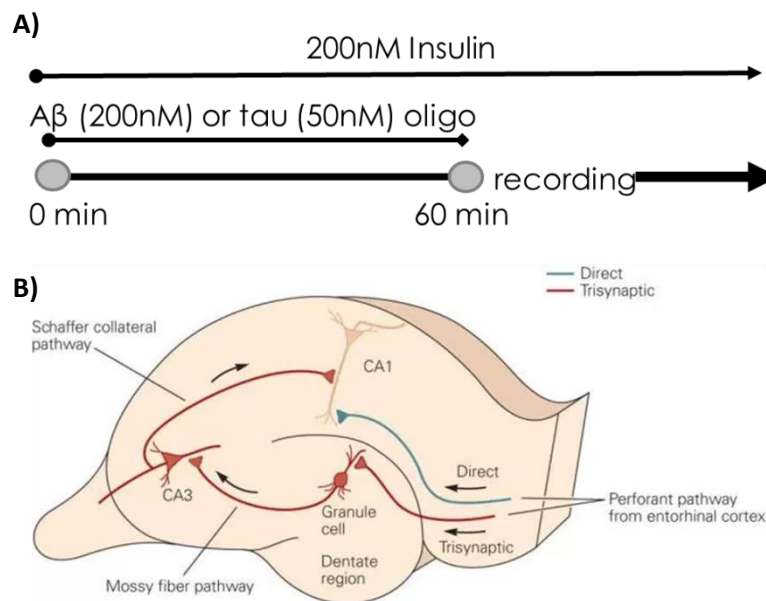
Figure 15: Electrophysiology Experimental Design. A) Oligomer challenge paradigm for electrophysiological assessment of LTP suppression. B) Hippocampal slice schematic of various neural pathways. Electrophysiological recording of the Schaffer collateral pathway was performed by stimulating at the CA3 and recording from the CA1 region.

I saw a reduction in the magnitude of LTP from untreated brain slices in both the ipsilateral and contralateral hippocampi from the injured animals' vs sham animals at 1MPI. At 3 MPI, I found this same significant reduction in the magnitude of LTP from untreated brain slices from the injured animals' vs sham animals in the ipsilateral hippocampus only.
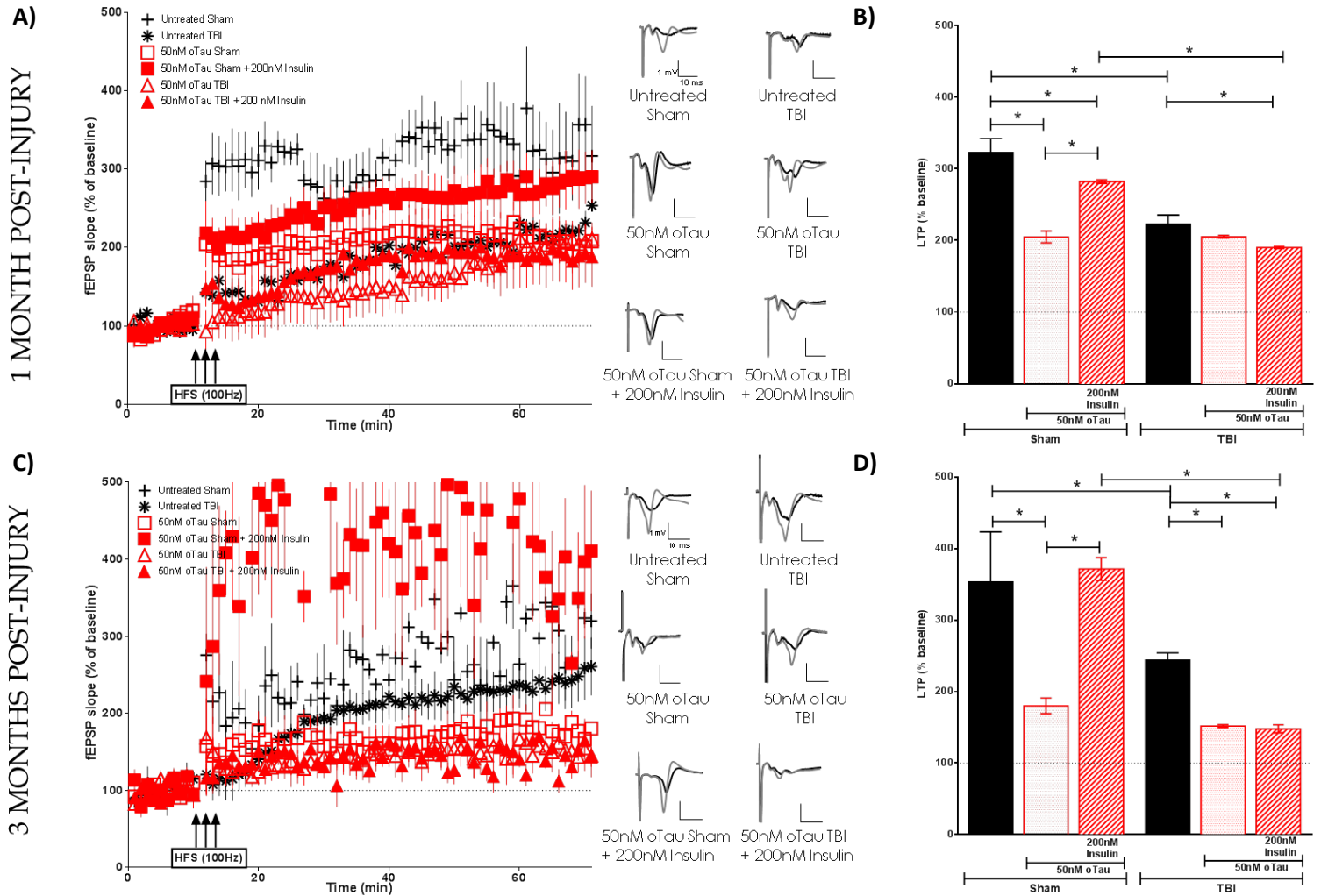
In slices treated with Aβ oligomers for 1 hour prior to recording, the magnitude of LTP was significantly lower in the TBI versus sham group in the ipsilateral hippocampus at 1 MPI (Figure 16B). However, in the contralateral hippocampus, we saw the opposite effect where the magnitude of LTP, while only modestly higher, was significantly increased compared to slices from sham animals when treated with Aβ (Figure 18B). For tau oligomer-treated slices at 1 MPI, the magnitude of LTP was significantly decreased in slices taken from TBI versus sham animals in the contralateral hippocampus only (Figure 19B). However, for 3 MPI, in both hemispheres' hippocampi, we found no significant differences in LTP suppression due to either the Aβ (Figure 16D and Figure 18D) or tau oligomer (Figure 17D and Figure 19D) treatments for the TBI versus sham group.

The 200nM insulin treatment during both the Aβ and tau oligomer-challenge was able to block LTP suppression in sham hippocampal slices at both time points in the ipsilateral (Figure 16B/D and Figure 17B/D) and contralateral hemispheres (Figure 18B/D and Figure 19B/D). Interestingly, the insulin treatment did not block the Aβ-induced LTP inhibition in slices from TBI animals in any of our groups (Figure 16B/D and Figure 18B/D). While the insulin provided no protection against the tau-induced LTP reduction in slices from TBI animals in the ipsilateral hemisphere (Figure 17B/D), we did find that insulin provided a partial protection against tau in the contralateral hemisphere at both time points (Figure 19B/D). Importantly, in slices treated with insulin alone

(Figure 20), insulin did not enhance LTP expression in SHAM nor in TBI animals in either hemisphere.
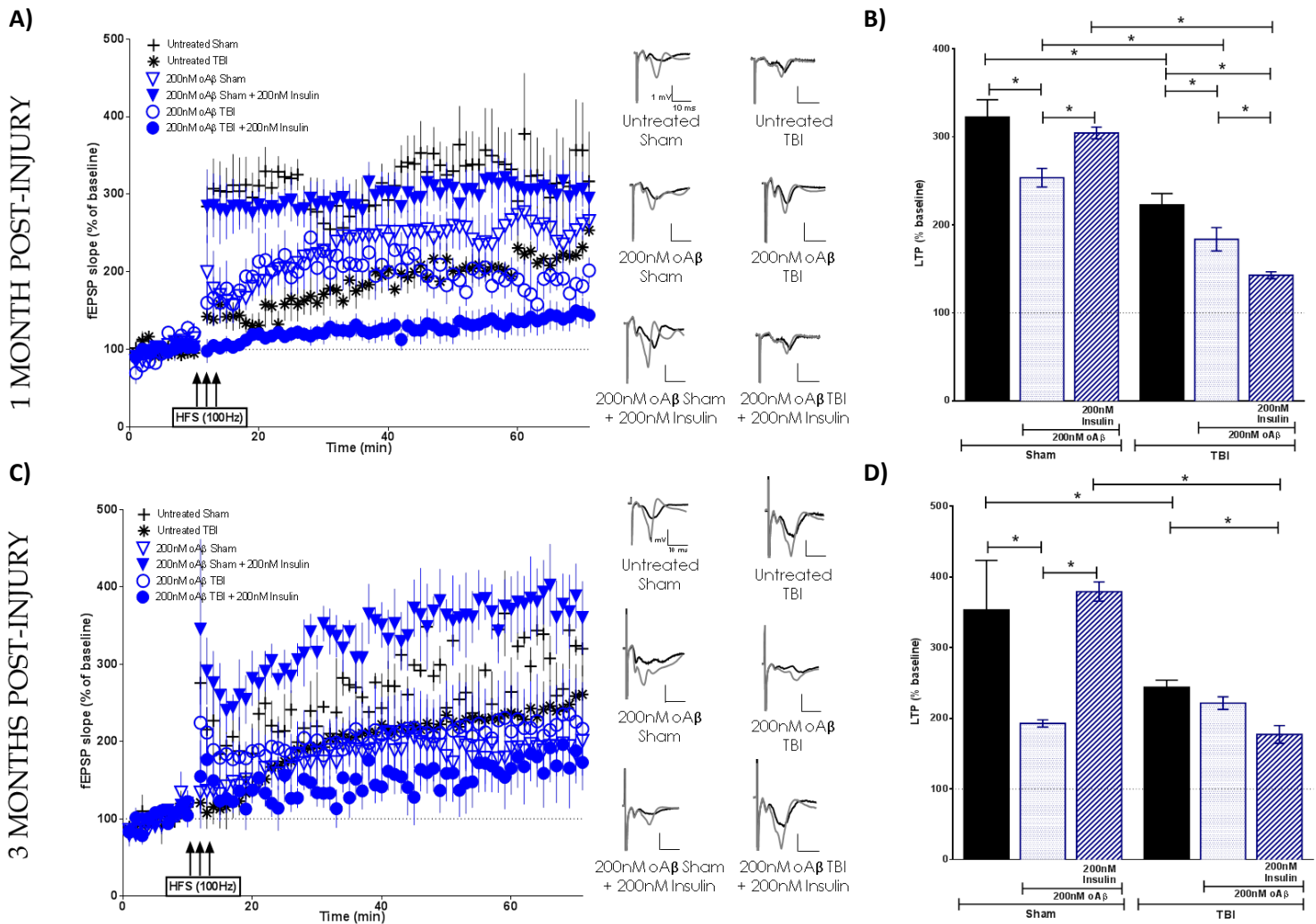
Figure 16: Electrophysiological Analysis of Aβ Oligomer-Treatment in Ipsilateral Hippocampus. Schaffer collateral field recordings were performed to determine oligomer-induced LTP impairment in slices from sham and TBI animals. Graphs of fEPSP's slopes as a percentage of the baseline with representative traces for each condition at A) 1 month post-injury and C) 3 months post-injury. Graphs showing the average of the fEPSP slope for the final 10 minutes (time points 60-70 minutes post high frequency stimulation) as an indication of LTP for each condition at B) 1 month post-injury and D) 3 months post-injury. 1 MPI n= 4 animals and 3-6 slices per condition; 3 MPI n= 3-5 animals and 3-7 slices per condition. One way ANOVA with Bonferroni's post hoc analysis was used to determine statistical significance. Error bars represent standard deviation. *p < 0.05

Figure 17: Electrophysiological Analysis of Tau Oligomer-Treatment in Ipsilateral Hippocampus. Schaffer collateral field recordings were performed to determine oligomer-induced LTP impairment in slices from sham and TBI animals. Graphs of fEPSP's slopes as a percentage of the baseline with representative traces for each condition at A) 1 month post-injury and C) 3 months post-injury. Graphs showing the average of the fEPSP slope for the final 10 minutes (time points 60-70 minutes post high frequency stimulation) as an indication of LTP for each condition at B) 1 month post-injury and D) 3 months post-injury. 1 MPI n= 4 animals and 3-6 slices per condition; 3 MPI n= 3-5 animals and 3-7 slices per condition. One way ANOVA with Bonferroni's post hoc analysis was used to determine statistical significance. Error bars represent standard deviation. *$p < 0.05$
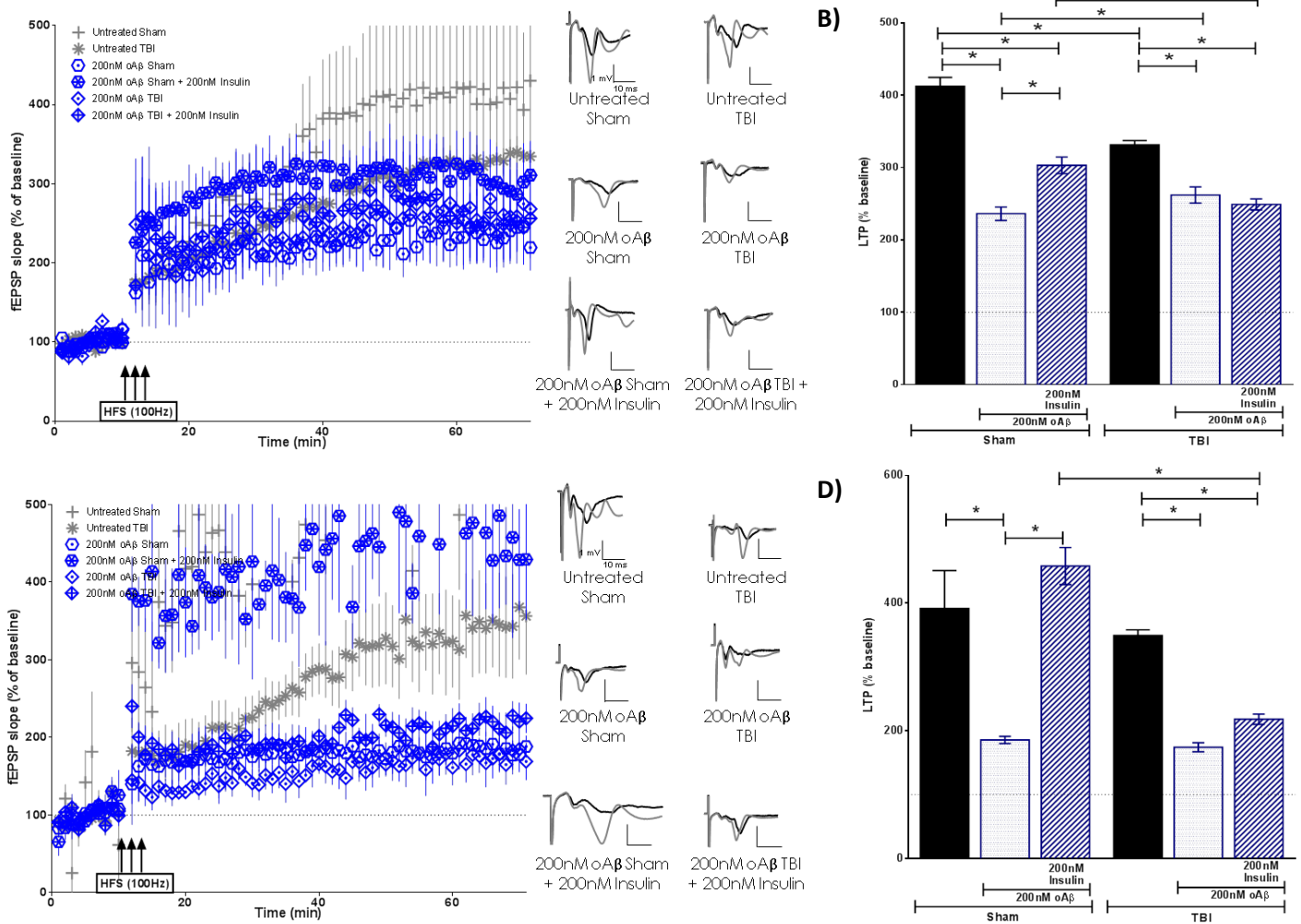
Figure 18: Electrophysiological Analysis of Aβ Oligomer-Treatment in Contralateral Hippocampus. Schaffer collateral field recordings were performed to determine oligomer-induced LTP impairment in slices from sham and TBI animals. Graphs of fEPSP's slopes as a percentage of the baseline with representative traces for each condition at A) 1 month post-injury and C) 3 months post-injury. Graphs showing the average of the fEPSP slope for the final 10 minutes (time points 60-70 minutes post high frequency stimulation) as an indication of LTP for each condition at B) 1 month post-injury and D) 3 months post-injury. 1 MPI n= 4 animals and 3-6 slices per condition; 3 MPI n= 3-5 animals and 3-7 slices per condition. One way ANOVA with Bonferroni's post hoc analysis was used to determine statistical significance. Error bars represent standard deviation. *p < 0.05
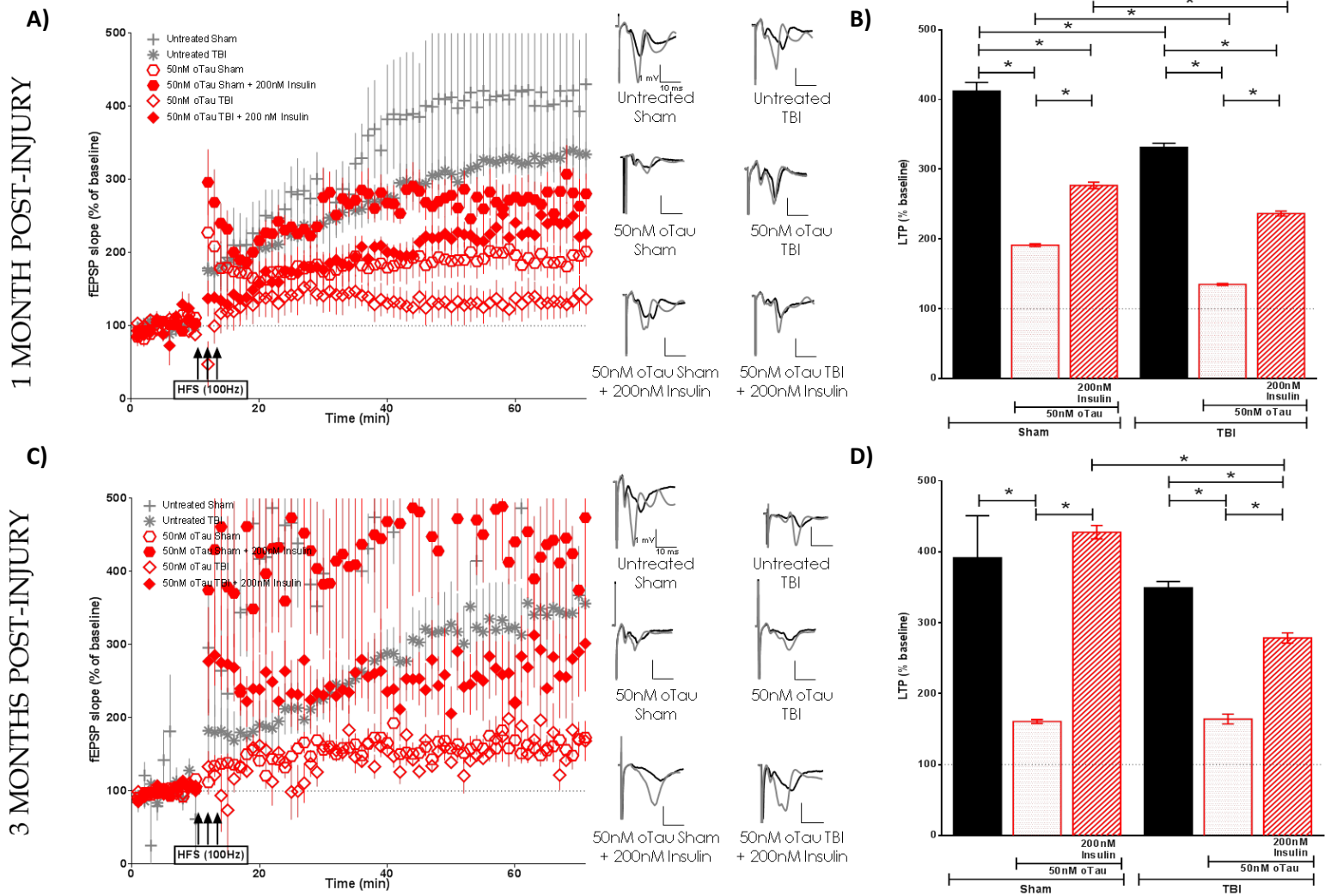
Figure 19: Electrophysiological Analysis of Tau Oligomer-Treatment in Contralateral Hippocampus. Schaffer collateral field recordings were performed to determine oligomer-induced LTP impairment in slices from sham and TBI animals. Graphs of fEPSP's slopes as a percentage of the baseline with representative traces for each condition at A) 1 month post-injury and C) 3 months post-injury. Graphs showing the average of the fEPSP slope for the final 10 minutes (time points 60-70 minutes post high frequency stimulation) as an indication of LTP for each condition at B) 1 month post-injury and D) 3 months post-injury. 1 MPI n= 4 animals and 3-6 slices per condition; 3 MPI n= 3-5 animals and 3-7 slices per condition. One way ANOVA with Bonferroni's post hoc analysis was used to determine statistical significance. Error bars represent standard deviation. *$p < 0.05$

A) **B)**

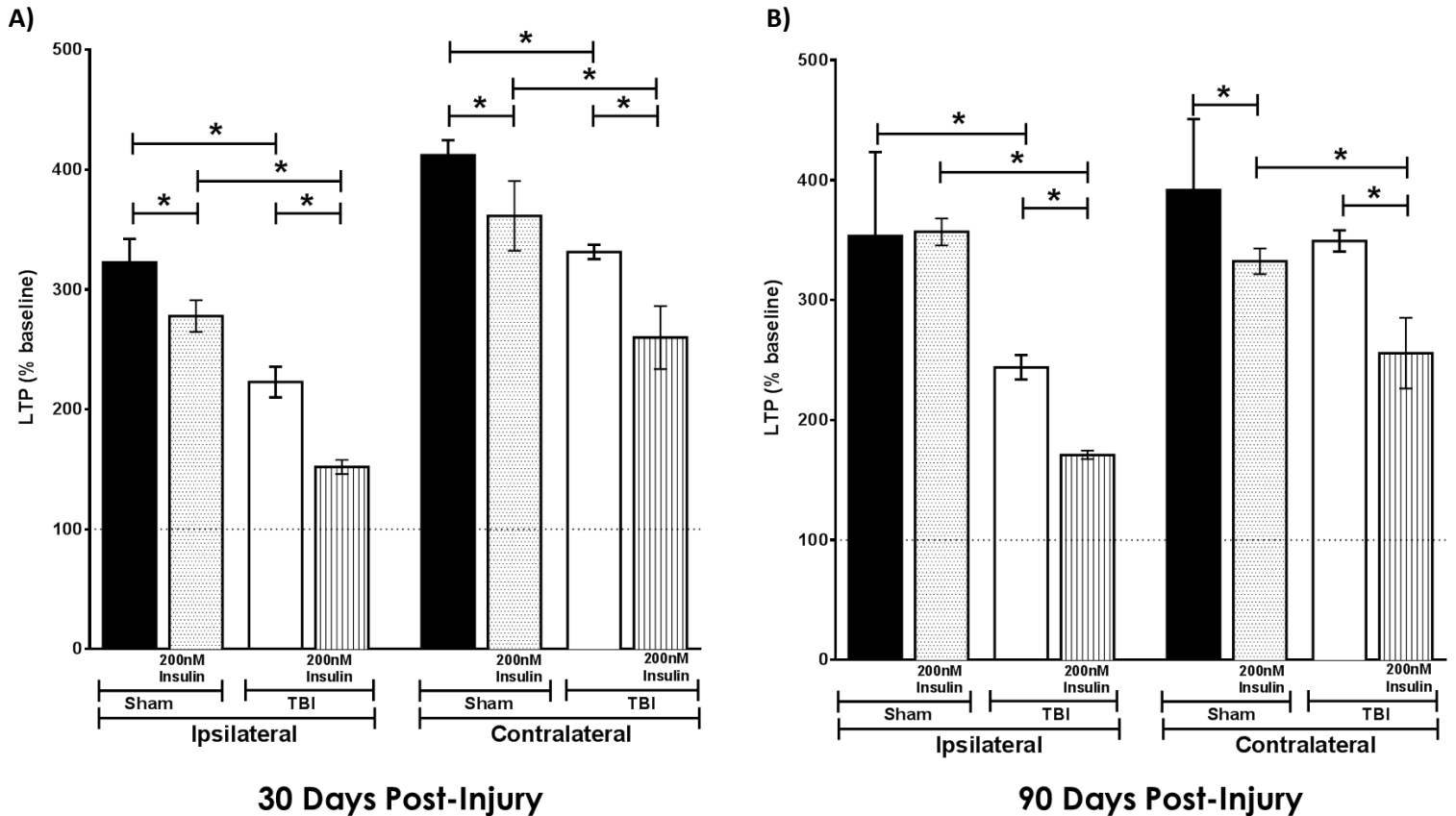**30 Days Post-Injury** **90 Days Post-Injury**

Figure 20: Electrophysiological Analysis of Insulin-Treatment Alone in Ipsilateral and Contralateral Hippocampi. Schaffer collateral field recordings were performed to determine the effect of a 200nM insulin treatment on LTP in slices from sham and TBI animals. Graphs showing the average of the fEPSP slope for the final 10 minutes (time points 60-70 minutes post high frequency stimulation) as an indication of LTP at A) 1 month post-injury and B) 3 months post-injury. 1 MPI n= 4 animals and 3-6 slices per condition; 3 MPI n= 3-5 animals and 3-7 slices per condition. One way ANOVA with Bonferroni's post hoc analysis was used to determine statistical significance. Error bars represent standard deviation. $*p < 0.05$

In summary, my results are consistent with those demonstrated by multiple groups showing that TBI results in impaired LTP, specifically in the hemisphere of injury (ipsilateral). Collectively, my results suggest that TBI does not generally affect vulnerability of synapses to Aβ or tau oligomer-induced LTP impairments to a higher degree from that seen in sham animals at 1 or 3 months after injury. Importantly though, the concurrence of insulin treatment with either of the oligomer challenges on hippocampal slices blocked the LTP impairment in both ipsilateral and contralateral slices from sham animals. This beneficial effect was not seen for either Aβ or tau in

54

the ipsilateral hippocampus of TBI animals at either time point as well as for Aβ impairment at either time point in the contralateral hippocampus. This data further corroborates the insulin resistance in the hippocampus after TBI shown by the *ex vivo* insulin stimulation analysis previously described and provides a valuable demonstration that even a significant administration of insulin cannot overcome this phenomenon to provide a protection that is normally afforded by insulin.

<u>What could be causing the benefit in LTP by insulin in the presence of oligomers?</u>

Although my *ex vivo* binding studies as well as the electrophysiology results did not suggest that there is an increase in oligomer binding after TBI, to try and determine why insulin treatment was able to block the Aβ-induced LTP depression in sham animals but not TBI animals, I wanted to determine if this insulin treatment normally decreased the amount of Aβ binding in similar conditions as those used for my electrophysiological experiments. To accomplish this, I used brain slices from naïve, wild-type rats and challenged with 2.5μM Aβ-oligomers with or without 200nM insulin for 1 hour at 37°C in an aerated tissue incubator, and I assessed Aβ-binding using flow cytometry on synaptosomes isolated from these slices (Figure 21). I did not detect any change in Aβ-binding using insulin treatment with this paradigm. Thus, the insulin phenomenon of blocking an Aβ-induced deficit in LTP in sham animals but not TBI animals cannot be explained by a decrease in Aβ-binding. Rather, this phenomenon may just be due to a more functionally resilient synapse of uninjured animals.
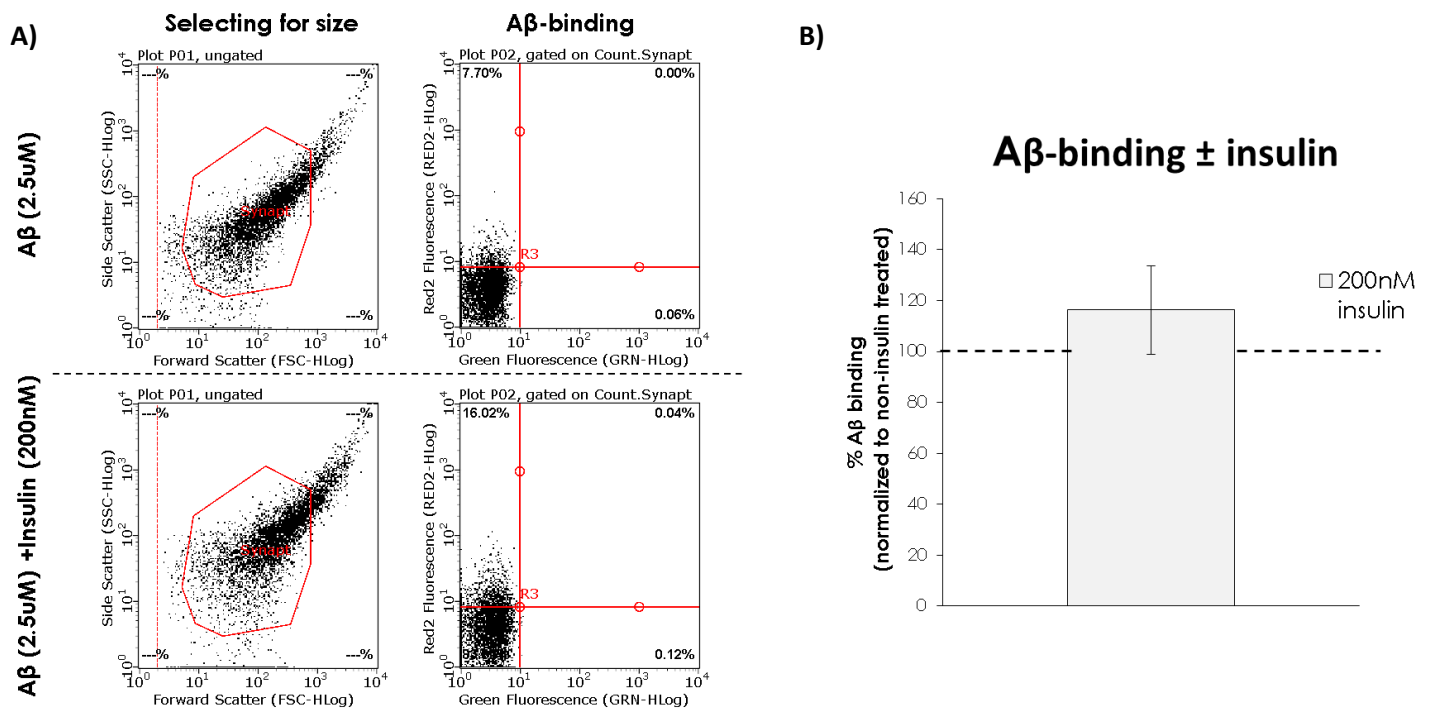
Figure 21: Insulin's Effect on Aβ Binding. Brain slices from naïve, wild-type rats were challenged with 2.5μM Aβ-oligomers ± 200nM insulin for 1 hour to mimic the insulin stimulation used for the electrophysiology paradigm. A) Representative flow cytometry size gating and fluorescence of the Aβ-binding analysis performed on synaptosomes isolated from these slices. B) Quantification revealed no changes in Aβ-binding using insulin treatment with this paradigm. Graph representing mean ± SEM. N=4 animals total, 11 slices per condition.

In a second attempt to investigate a possible mechanism to explain the resilience of sham animals compared to TBI animals in my electrophysiological results, I wanted to determine if insulin is able to change or enhance synaptic mitochondrial function and/or number using the same electrophysiological paradigm. I performed this experiment on brain slices from naïve, wild-type rats and stimulated slices for 1 hour at 37°C in an aerated tissue incubator with 200nM or 2.5μM insulin. I then isolated synaptosomes, labeled mitochondria, and analyzed mitochondrial membrane potential (Mitosense) and mitochondrial count (Mitotracker) using flow cytometry (Figure 22). Neither insulin treatment condition resulted in any mitochondrial changes in mitochondrial membrane potential or mitochondrial number versus insulin unstimulated slices;

therefore, mitochondrial stimulation from insulin is not a mechanism that would be able to explain

insulin's ability to block oligomer-induced LTP suppression in sham but not TBI animals.
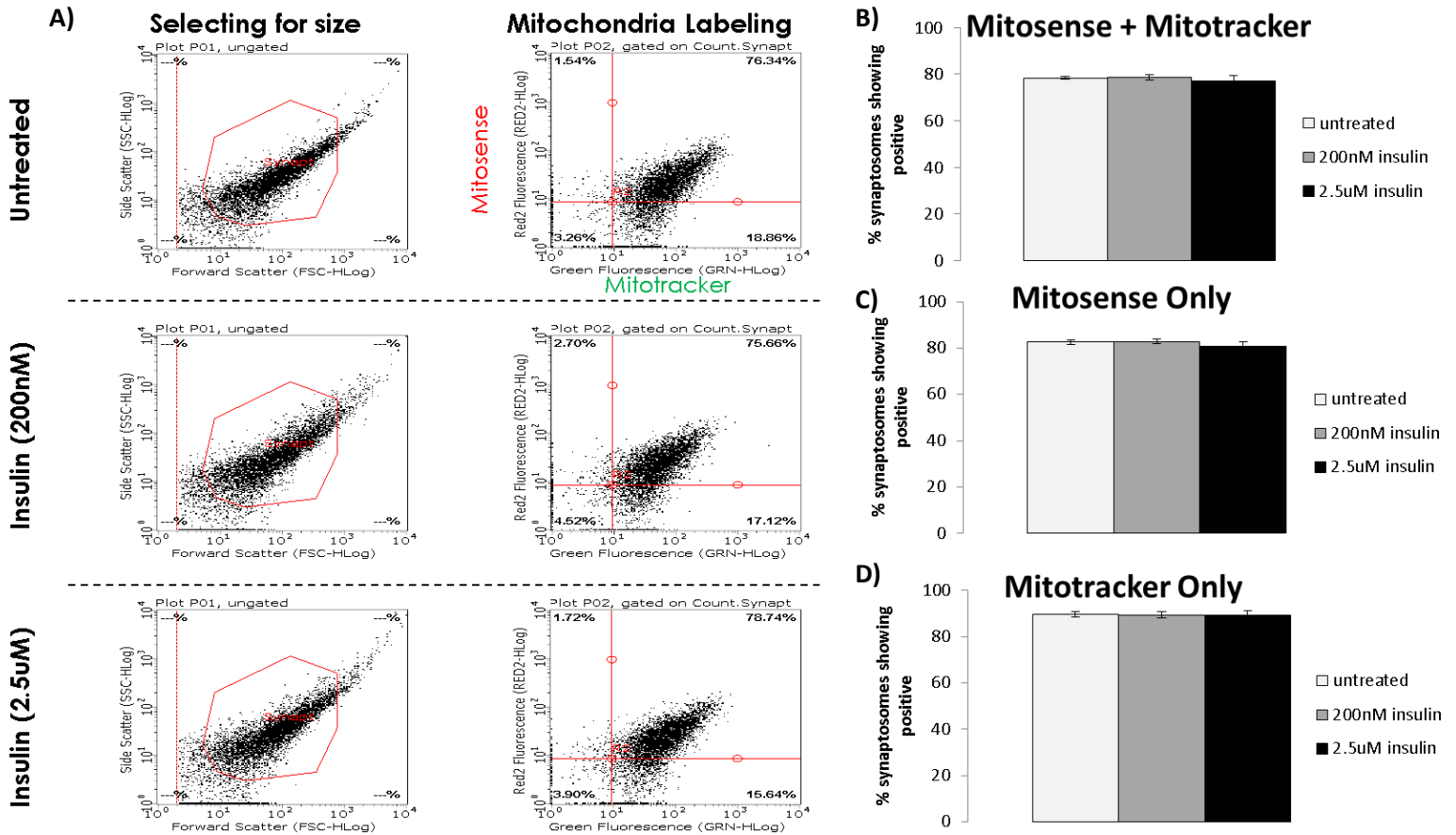
Figure 22: Mitochondria Analysis after Insulin Stimulation. Brain slices from naïve, wild-type rats were treated with either 200nM or 2.5µM of insulin for 1 hour to mimic the insulin stimulation used for the electrophysiology paradigm. A) Representative flow cytometry size gating and fluorescence of mitochondrial dyes on synaptosomes isolated from these slices. Quantification revealed no changes in B) mitochondria double labeled for Mitosense and Mitotracker, C) mitochondria analyzed for Mitosense alone, or D) mitochondria analyzed for Mitotracker alone indicating that neither insulin concentration altered mitochondria potential or mitochondria number using this paradigm. Graphs representing mean ± SEM. Untreated n=10 slices, 200nM insulin n=10 slices, 2.5uM insulin n=9 slices. N=3 animals total.

Discussion

TBI increases the risk of developing AD later in life[36]. Synaptic dysfunction caused by toxic Aβ and tau oligomeric species binding to the synapse and disrupting LTP properties is one of the initial events in AD leading to the cognitive decline that is associated with this disease[15,16]. Moreover, insulin signaling plays a role in synaptic health and function[41], and disruption of this normal functioning through insulin resistance at the synapse has been shown to contribute to Aβ-induced spine loss in AD[40,43]. Thus, the main goal of this project was to 1) determine whether synaptic insulin responsiveness after TBI is dysregulated/ decreased and to 2) investigate related changes in synaptic vulnerability (including association to and functional disruption of synapses) to Aβ and tau oligomers.

In this study, I used a moderate fluid-percussion injury (FPI) TBI model in rats to first determine if there were alterations in synaptic insulin responsiveness in the hippocampus at 2 days post-injury (DPI), 7 DPI, 1-month post-injury (MPI), and 3 MPI. I employed an *ex vivo* insulin stimulation method on isolated synaptosomes to directly assess insulin responsiveness of the insulin receptor (IR) and found the synaptic IR to have significantly decreased responsiveness as early as 7 DPI after lateral FPI. This hippocampal insulin resistance demonstrated chronic deficits in synaptic insulin responsiveness up to my latest time point of 3 MPI in hippocampi from both hemispheres.

Further analysis of this data was able to give additional insights into this phenomenon. In the ipsilateral hippocampus, my results revealed a significant increase in IR level at 3 MPI at the synapse which could be indicative of an attempted compensatory mechanism for the decreased insulin signaling here. However, these possible efforts were shown to be futile as I found that there is still a significantly decreased synaptic insulin response as well as decreased basal

58

phosphorylation levels at this time point indicating that there is a chronic alteration in the response of the receptor that cannot be overcome by upregulation of the receptor. Furthermore, I did not find any changes in synaptic IR level at any of the time points for the contralateral hemisphere. This difference may be indicative of differing mechanisms driving the insulin resistance for the opposing brain hemispheres, and these experiments prompted brief mechanistic experiments to investigate possible drivers of this insulin resistance differences.

I only looked at a single protein, SOCS3, which can act directly on the insulin receptor to see if it could possibly be involved in initiating the synaptic insulin resistance after TBI that I saw. SOCS3 is a protein of the suppressor of cytokine signaling (SOCS) family that act as negative regulators of cytokine and growth factor signaling. SOCS3 protein expression can be induced by IL6 as well as IL10 and has been shown to negatively regulate insulin signaling[75] and is, in fact, upregulated in AD[76]. To investigate whether the protein SOCS3 could be playing a role in the synaptic insulin resistance I saw in my TBI model, I looked at the level of this protein in isolated synaptosomes from the ipsilateral and contralateral hippocampi at our 2 DPI, 7 DPI, 1 MPI, and 3 MPI time points.

In the ipsilateral hippocampus, I found a significantly increased level of SOCS3 at the synapse in TBI animals versus sham animals beginning at 2 DPI through 1 MPI. Since this occurs prior to insulin resistance that my previous data showed at the synapse starting at 7DPI, this could potentially be a driving factor in initiating the dysregulation and insulin resistance. This upregulation could be a link between the chronic inflammation seen after TBI[50,77] and the insulin resistance that I have reported here in hippocampal synapses after injury.

In the contralateral hemisphere, however, I did not find altered levels of SOCS3 at the synapse at any of the time points. While I still found synaptic insulin resistance beginning at 7DPI in this hemisphere too, this finding is a second difference between the opposing hippocampi that is suggestive of the two hemispheres resulting in insulin resistance from differing mechanisms. Perhaps SOCS3 plays a role in the ipsilateral hemisphere while the alterations in insulin responsiveness in the ipsilateral hemisphere then drive the changes in the contralateral hemisphere. Additionally, alternative proteins that directly bind to the insulin receptor that we did not investigate in this study may be involved in the contralateral hemisphere's insulin resistance. This would not be surprising as many TBI consequences have been shown in the literature to have different mechanisms driving the alterations for each hemisphere since the injury given is a lateral injury. However, to adequately determine a mechanism driving synaptic insulin resistance after TBI, many more in depth studies will need to be performed looking at a multitude of other proteins including alternative SOCS proteins, PTP1B, and Grb10/Grb14 adaptor proteins[75].

After characterizing synaptic insulin receptor responsiveness, I aimed to determine if there is altered synaptic resistance to the association of extracellular Aβ and tau oligomers using *ex vivo* binding methodologies. My data indicates that this chronic decreased insulin responsiveness at the synapse does not lead to an increased susceptibility to either Aβ or tau oligomer binding in hippocampal synapses at the intermediate and chronic time points of 1 month or 3 months after moderate FPI.

I further investigated the impact of Aβ and tau oligomers on synaptic function through long-term potentiation (LTP) in these late time points and determined whether insulin treatment was able to alleviate this oligomer-induced LTP disruption.

I did find basal LTP levels to be chronically impaired in the side of injury after TBI at both 1 and 3 MPI. However, my electrophysiological results suggest that overall synaptic vulnerability to Aβ and tau oligomer-induced LTP impairments is not increased after TBI compared to sham animals at 1 or 3 months after injury. To explore the relationship between synaptic dysfunction due to the oligomers and the hippocampal synaptic insulin resistance I found in my previous data, I additionally evaluated oligomer-induced LTP suppression with the addition of a co-incubation insulin treatment. Consistent with previous work showing that insulin treatment increases synaptic resilience to AD pathology[43], I found that insulin treatment provides protection against Aβ and tau-induced LTP functional impairments in sham animals. However, in ipsilateral hippocampal slices from TBI animals, this beneficial effect of insulin was not seen against either Aβ or tau at either 1 or 3 MPI. Insulin treatment also did not block Aβ impairment at either time point in the contralateral hippocampus. We did find that insulin treatment partially blocked LTP reduction due to tau oligomers in the contralateral hippocampus at both chronic time points, yet I do not have an explanation for this phenomenon.

I performed a couple experiments in an attempt to explain how insulin is able to alleviate oligomer-induced LTP suppression in the sham animals in a hope that this would lead me to investigate if these mechanisms were impaired in TBI animals. However, even under standard conditions (using naïve rats), I did not find that insulin was able to block or reduce Aβ oligomer binding in hippocampal slices with this paradigm. While the work published under Dr. De Felice has demonstrated that insulin can block Aβ binding in hippocampal cultures, I have not been able to find this demonstration using either *ev vivo* slices or *in vivo*. My second attempt at an explanation evaluated whether insulin could stimulate mitochondria which could possibly cause a functional increase in cell health, thus providing a phenomena to investigate in TBI animals. This attempt

also proved unsuccessful as I did not find any mitochondrial changes after an insulin treatment in naïve hippocampal slices using this paradigm. A third possibility involves the property of insulin to recruit NMDA receptors to the membrane that has previously been described. For this scenario, rather than blocking the LTP-suppression by oligomers, insulin could be involved in a compensatory mechanism that we are seeing as an increase in LTP. However, my electrophysiology data on insulin treatment alone on sham hippocampal slices suggests otherwise since insulin treatment either did not affect or, in some cases, even significantly decreased LTP. Therefore, I still do not have a mechanistic explanation as to the beneficial effect seen by insulin on the LTP suppression by oligomers. Further hypothesis and experiments need to be performed to give insight into this mechanism.

Overall, my results demonstrate that the insulin-resistant induced state after traumatic brain injury is now unresponsive to the beneficial effect of insulin therapy as a treatment against impairments due to AD-pathology. This work demonstrates the importance of having refined treatments for AD based on a history of risk factors and demonstrates how these risk factors may impact the efficacy of particular treatments that are being investigated for AD in the general population.

Conclusions and Future Directions

From my electrophysiology data as well as my *ex vivo* insulin stimulation analysis, I found chronically decreased insulin responsiveness of the synaptic insulin receptor in the hippocampus after moderate TBI in rats. While I did not find an increased synaptic susceptibility to Aβ or tau in this model, my data exemplified that a significant administration of insulin cannot overcome this resistance to provide a protection against oligomer-induced synaptic dysfunction that is normally provided by insulin under standard conditions. Therefore, there is high translational value in the therapeutic implications of this research establishing that this insulin-resistant induced state after TBI is now unresponsive to the beneficial effect of insulin therapy as a treatment against impairments due to AD-pathology. Thus, AD patients may need to have refined treatments based on their prior history of associated risk factors. Further work examining the mechanistic drivers of TBI-induced insulin resistance will provide important insights into upstream targets for potential therapies to halt TBI insult progression and exacerbation of consequences.

References

1.   Alzheimer's Association. *2018 Alzheimer's Disease Facts and Figures Includes a Special Report on the Financial and Personal Benefits of Early Diagnosis*. Vol 14.; 2018. doi:10.1016/j.jalz.2016.03.001

2.   Strassnig M, Ganguli M. About a Peculiar Disease of the Cerebral Cortex: Alzheimer's Orignial Case Revisited. *Psychiatry*. 2005;September:30-33. https://www.ncbi.nlm.nih.gov/pmc/articles/PMC2993534/pdf/PE_2_9_30.pdf. Accessed November 2, 2018.

3.   Selkoe DJ, Hardy J. The amyloid hypothesis of Alzheimer's disease at 25 years. *EMBO Mol Med*. 2016;8(6):595-608. doi:10.15252/emmm.201606210

4.   Baumgart M, Snyder HM, Carrillo MC, Fazio S, Kim H, Johns H. Summary of the evidence on modifiable risk factors for cognitive decline and dementia: A population-based perspective. *Alzheimer's Dement*. 2015;11(6):718-726. doi:10.1016/j.jalz.2015.05.016

5.   Querfurth HW, Laferla FM. Alzheimer's disease. *N Engl J Med*. 2010;362(4):329-344. doi:10.1056/NEJMra0909142

6.   Sachdev PS, Blacker D, Blazer DG, et al. Classifying neurocognitive disorders: The DSM-5 approach. *Nat Rev Neurol*. 2014;10(11):634-642. doi:10.1038/nrneurol.2014.181

7.   Yaari R, Corey-Bloom J. Alzheimer's Disease. *Semin Neurol*. 2007;27(1):32-41. doi:10.1055/s-2006-956753

8.   Selkoe DJ. Alzheimer's Disease: Genes, Proteins, and Therapy. *Physiol Rev*. 2001;81(2):741-766. http://physrev.physiology.org. Accessed November 9, 2018.

9. Haass C, Kaether C, Thinakaran G, Sisodia S. Trafficking and proteolytic processing of APP. *Cold Spring Harb Perspect Med*. 2012;2(5):a006270. doi:10.1101/cshperspect.a006270

10. Kang J, Lemaire HG, Unterbeck A, et al. The precursor of Alzheimer's disease amyloid A4 protein resembles a cell-surface receptor. *Nature*. 1987;325(6106):733-736. doi:10.1038/325733a0

11. Wang Y, Mandelkow E. Tau in physiology and pathology. *Nat Rev Neurosci*. 2016;17(1):5-21. doi:10.1038/nrn.2015.1

12. Buée L, Bussière T, Buée-Scherrer V, Delacourte A, Hof PR. Tau protein isoforms, phosphorylation and role in neurodegenerative disorders. *Brain Res Rev*. 2000;33(1):95-130. doi:10.1016/S0165-0173(00)00019-9

13. Ross CA, Poirier MA. What is the role of protein aggregation in neurodegeneration? *Nat Rev Mol Cell Biol*. 2005;6(11):891-898. doi:10.1038/nrm1742

14. Kotler SA, Walsh P, Brender JR, Ramamoorthy A. Differences between amyloid-β aggregation in solution and on the membrane: Insights into elucidation of the mechanistic details of Alzheimer's disease. *Chem Soc Rev*. 2014;43(19):6692-6700. doi:10.1039/c3cs60431d

15. Fá M, Puzzo D, Piacentini R, et al. Extracellular Tau Oligomers Produce An Immediate Impairment of LTP and Memory. *Sci Rep*. 2016;6. doi:10.1038/srep19393

16. Puzzo D, Piacentini R, Fá M, et al. LTP and memory impairment caused by extracellular Aβ and tau oligomers is APP- dependent. *Elife*. 2017;6. doi:10.7554/eLife.26991.001

17. Kayed R, Head E, Thompson JL, et al. Common Structure of Soluble Amyloid Oligomers

Implies Common Mechanism of Pathogenesis. *Science (80-)*. 2003;300:486-489. doi:10.1126/science.289.5483.1317

18.   Knowles TPJ, Vendruscolo M, Dobson CM. The amyloid state and its association with protein misfolding diseases. *Nat Rev Mol Cell Biol*. 2014;15(6):384-396. doi:10.1038/nrm3810

19.   Spires-Jones TL, Attems J, Thal DR. Interactions of pathological proteins in neurodegenerative diseases. *Acta Neuropathol*. 2017;134(2):187-205. doi:10.1007/s00401-017-1709-7

20.   Lacor PN, Buniel MC, Chang L, et al. Synaptic Targeting by Alzheimer's-Related Amyloid beta Oligomers. *Neurobiol Dis* . 2004;24(45):10191-10200. doi:10.1523/JNEUROSCI.3432-04.2004

21.   Lacor PN, Buniel MC, Furlow PW, et al. Amyloid beta Oligomer-Induced Aberrations in Synapse Composition, Shape, and Density Provide a Molecular Basis for Loss of Connectivity in Alzheimer's Disease. *Neurobiol Dis*. 2007;27(4):796-807. doi:10.1523/JNEUROSCI.3501-06.2007

22.   Spires TL, Meyer-Luehmann M, Stern EA, et al. Neurobiology of Disease Dendritic Spine Abnormalities in Amyloid Precursor Protein Transgenic Mice Demonstrated by Gene Transfer and Intravital Multiphoton Microscopy. *J Neurosci*. 2005;25(31):7278-7287. doi:10.1523/JNEUROSCI.1879-05.2005

23.   Zhao D, Watson JB, Xie C-W, Xie Amyloid C-W. Amyloid Prevents Activation of Calcium/Calmodulin-Dependent Protein Kinase II and AMPA Receptor Phosphorylation During Hippocampal Long-Term Potentiation. *J Neurophysiol*. 2004;92:2853-2858.

doi:10.1152/jn.00485.2004

24.   Dineley KT, Kayed R, Neugebauer V, et al. Amyloid-β oligomers impair fear conditioned
       memory in a calcineurin-dependent fashion in mice. *J Neurosci Res*. 2010;88(13):2923-
       2932. doi:10.1002/jnr.22445

25.   Wu H-Y, Hudry E, Hashimoto T, et al. Amyloid   Induces the Morphological
       Neurodegenerative Triad of Spine Loss, Dendritic Simplification, and Neuritic
       Dystrophies through Calcineurin Activation. *J Neurosci*. 2010;30(7):2636-2649.
       doi:10.1523/JNEUROSCI.4456-09.2010

26.   Mohmmad Abdul H, Baig I, LeVine H, Guttmann RP, Norris CM. Proteolysis of
       calcineurin is increased in human hippocampus during mild cognitive impairment and is
       stimulated by oligomeric Abeta in primary cell culture. *Aging Cell*. 2011;10(1):103-113.
       doi:10.1111/j.1474-9726.2010.00645.x

27.   Terry RD, Masliah E, Salmon DP, et al. Physical basis of cognitive alterations in
       alzheimer's disease: Synapse loss is the major correlate of cognitive impairment. *Ann
       Neurol*. 1991;30(4):572-580. doi:10.1002/ana.410300410

28.   Spires-Jones TL, Hyman BT. The intersection of amyloid beta and tau at synapses in
       Alzheimer's disease. *Neuron*. 2014;82(4):756-771. doi:10.1016/j.neuron.2014.05.004

29.   Masters CL, Bateman R, Blennow K, Rowe CC, Sperling RA, Cummings JL. Alzheimer's
       disease. *Nat Rev Dis Prim*. 2015;1:15056. doi:10.1038/nrdp.2015.56

30.   Veitch D, Friedl K, Weiner M. Military Risk Factors for Cognitive Decline, Dementia and
       Alzheimer's Disease. *Curr Alzheimer Res*. 2013;10(9):907-930.
       doi:10.2174/15672050113109990142

31.   Campdelacreu J. Parkinson's disease and Alzheimer disease: environmental risk factors. *Neurol (English Ed*. 2014;29(9):541-549. doi:10.1016/j.nrleng.2012.04.022

32.   Blázquez E, Velázquez E, Hurtado-Carneiro V, Ruiz-Albusac JM. Insulin in the brain: Its pathophysiological implications for states related with central insulin resistance, type 2 diabetes and alzheimer's disease. *Front Endocrinol (Lausanne)*. 2014;5(OCT). doi:10.3389/fendo.2014.00161

33.   De La Monte SM. *Brain Insulin Resistance and Deficiency as Therapeutic Targets in Alzheimer's Disease*. Vol 9.; 2012. https://www.ncbi.nlm.nih.gov/pmc/articles/PMC3349985/pdf/CAR-9-35.pdf. Accessed September 28, 2018.

34.   Fleminger S, Oliver DL, Lovestone S, Rabe-Hesketh S, Giora A. Head injury as a risk factor for Alzheimer's disease: The evidence 10 years on; a partial replication. *J Neurol Neurosurg Psychiatry*. 2003;74(7):857-862. doi:10.1136/jnnp.74.7.857

35.   Tran HT, LaFerla FM, Holtzman DM, Brody DL. Controlled Cortical Impact Traumatic Brain Injury in 3xTg-AD Mice Causes Acute Intra-Axonal Amyloid- Accumulation and Independently Accelerates the Development of Tau Abnormalities. *J Neurosci*. 2011;31(26):9513-9525. doi:10.1523/JNEUROSCI.0858-11.2011

36.   Washington PM, Villapol S, Burns MP. Polypathology and dementia after brain trauma: Does brain injury trigger distinct neurodegenerative diseases, or should they be classified together as traumatic encephalopathy? *Exp Neurol*. 2016;275:381-388. doi:10.1016/j.expneurol.2015.06.015

37.   Swerdlow RH, Khan SM. The Alzheimer ' s disease mitochondrial cascade hypothesis :

An update. *Exp Neurol*. 2009;218(2):308-315. doi:10.1016/j.expneurol.2009.01.011

38.   Reddy PH, Manczak M, Mao P, Calkins MJ, Reddy AP, Shirendeb U. Amyloid-β and mitochondria in aging and Alzheimer's disease: Implications for synaptic damage and cognitive decline. *J Alzheimer's Dis*. 2010;20(SUPPL.2). doi:10.3233/JAD-2010-100504

39.   Breunig JJ, Guillot-Sestier MV, Town T. Brain injury, neuroinflammation and Alzheimer's disease. *Front Aging Neurosci*. 2013;5(JUL). doi:10.3389/fnagi.2013.00026

40.   Zhao W-Q, De Felice FG, Fernandez S, et al. Amyloid beta oligomers induce impairment of neuronal insulin receptors. *FASEB J*. 2008;22(1):246-260. doi:10.1096/fj.06-7703com

41.   Zhao WQ, Alkon DL. Role of insulin and insulin receptor in learning and memory. *Mol Cell Endocrinol*. 2001;177(1-2):125-134. doi:10.1016/S0303-7207(01)00455-5

42.   Talbot K, Wang HY, Kazi H, et al. Demonstrated brain insulin resistance in Alzheimer's disease patients is associated with IGF-1 resistance, IRS-1 dysregulation, and cognitive decline. *J Clin Invest*. 2012;122(4):1316-1338. doi:10.1172/JCI59903

43.   De Felice FG, Vieira MNN, Bomfim TR, et al. Protection of synapses against Alzheimer's-linked toxins: Insulin signaling prevents the pathogenic binding of Aβ oligomers. *Proc Natl Acad Sci*. 2009;106(6):1971-1976. doi:10.1073/pnas.0809158106

44.   Reger MA, Watson GS, Green PS, et al. Intranasal insulin improves cognition and modulates β-amyloid in early AD. *Neurology*. 2008;70(6):440-448. doi:10.1212/01.WNL.0000265401.62434.36

45.   Rodriguez-Rivera J, Denner L, Dineley KT. Rosiglitazone reversal of Tg2576 cognitive deficits is independent of peripheral gluco-regulatory status. *Behav Brain Res*. 2011;216(1):255-261. doi:10.1016/j.bbr.2010.08.002

46.   Bedse G, Di Domenico F, Serviddio G, Cassano T. Aberrant insulin signaling in Alzheimer's disease: Current knowledge. *Front Neurosci*. 2015;9(MAY):204. doi:10.3389/fnins.2015.00204

47.   Taylor CA, Bell JM, Breiding MJ, Xu L. Traumatic Brain Injury–Related Emergency Department Visits, Hospitalizations, and Deaths — United States, 2007 and 2013. *MMWR Surveill Summ*. 2017;66(9):1-16. doi:10.15585/mmwr.ss6609a1

48.   Centers for Disease Control and Prevention. Traumatic Brain Injury and Concussion. https://www.cdc.gov/traumaticbraininjury/index.html. Accessed November 5, 2018.

49.   Chauhan NB. Chronic neurodegenerative consequences of traumatic brain injury. *Restor Neurol Neurosci*. 2014;32(2):337-365. doi:10.3233/RNN-130354

50.   Walker KR, Tesco G. Molecular mechanisms of cognitive dysfunction following traumatic brain injury. *Front Aging Neurosci*. 2013;5(JUL):29. doi:10.3389/fnagi.2013.00029

51.   Gentleman SM, Greenberg BD, Savage MJ, et al. A beta 42 is the predominant form of amyloid beta-protein in the brains of short-term survivors of head injury. *Neuroreport*. 1997;8(6):1519-1522. http://www.ncbi.nlm.nih.gov/pubmed/9172166. Accessed November 5, 2018.

52.   DeKosky ST, Abrahamson EE, Ciallella JR, et al. Association of Increased Cortical Soluble Aβ42 Levels With Diffuse Plaques After Severe Brain Injury in Humans. *Arch Neurol*. 2007;64(4):541. doi:10.1001/archneur.64.4.541

53.   Uryu K, Chen X-H, Martinez D, et al. Multiple Proteins Implicated in Neurodegenerative Diseases Accumulate in Axons After Brain Trauma in Humans. *Exp Neurol*.

2007;208(2):185-192. doi:10.1016/j.expneurol.2007.06.018

54.   Washington PM, Morffy N, Parsadanian M, Zapple DN, Burns MP. Experimental

        Traumatic Brain Injury Induces Rapid Aggregation and Oligomerization of Amyloid-Beta

        in an Alzheimer's Disease Mouse Model. *J Neurotrauma*. 2014;31(1):125-134.

        doi:10.1089/neu.2013.3017

55.   Graham DI, Gentleman SM, Nicoll JA, et al. Altered beta-APP metabolism after head

        injury and its relationship to the aetiology of Alzheimer's disease. *Acta Neurochir Suppl*.

        1996;66:96-102. http://www.ncbi.nlm.nih.gov/pubmed/8780805. Accessed November 5,

        2018.

56.   Blasko I, Beer R, Bigl M, et al. Experimental traumatic brain injury in rats stimulates the

        expression, production and activity of Alzheimer's disease b-secretase (BACE-1). *J

        Neural Transm*. 2004;111:523-536. doi:10.1007/s00702-003-0095-6

57.   Chen X-H, Siman R, Iwata A, Meaney DF, Trojanowski JQ, Smith DH. Long-term

        accumulation of amyloid-beta, beta-secretase, presenilin-1, and caspase-3 in damaged

        axons following brain trauma. *Am J Pathol*. 2004;165(2):357-371.

        http://www.ncbi.nlm.nih.gov/pubmed/15277212. Accessed November 5, 2018.

58.   Yu F, Zhang Y, Chuang D-M. Lithium reduces BACE1 overexpression, β amyloid

        accumulation, and spatial learning deficits in mice with traumatic brain injury. *J

        Neurotrauma*. 2012;29(13):2342-2351. doi:10.1089/neu.2012.2449

59.   Cerecedo-López CD, Kim-Lee JH, Hernandez D, Acosta SA, Borlongan C V. Insulin-

        associated neuroinflammatory pathways as therapeutic targets for traumatic brain injury.

        Med Hypotheses. 2014;82(2):171-174. doi:10.1016/j.mehy.2013.11.028

60.   Shi J, Dong B, Mao Y, et al. Review: Traumatic brain injury and hyperglycemia, a

potentially modifiable risk factor. *Oncotarget*. 2015;7(43):71052-71061.

doi:10.18632/oncotarget.11958

61.   Ley EJ, Srour MK, Clond MA, et al. Diabetic Patients With Traumatic Brain Injury:

Insulin Deficiency Is Associated With Increased Mortality. *J Trauma Inj Infect Crit Care*.

2011;70(5):1141-1144. doi:10.1097/TA.0b013e3182146d66

62.   Karelina K, Sarac B, Freeman LM, Gaier KR, Weil ZM. Traumatic brain injury and

obesity induce persistent central insulin resistance. *Eur J Neurosci*. 2016;43(8):1034-

1043. doi:10.1111/ejn.13194

63.   Sallam HS, Tumurbaatar B, Zhang WR, et al. Peripheral adipose tissue insulin resistance

alters lipid composition and function of hippocampal synapses. *J Neurochem*.

2015;133(1):125-133. doi:10.1111/jnc.13043

64.   Kabadi S V., Hilton GD, Stoica BA, Zapple DN, Faden AI. Fluid-percussion-induced

traumatic brain injury model in rats. *Nat Protoc*. 2010;5(9):1552-1563.

doi:10.1038/nprot.2010.112

65.   Franklin W, Taglialatela G. A method to determine insulin responsiveness in

synaptosomes isolated from frozen brain tissue. *J Neurosci Methods*. 2016;261:128-134.

doi:10.1016/j.jneumeth.2016.01.006

66.   Puig KL, Kulas JA, Franklin W, et al. The Ames dwarf mutation attenuates Alzheimer's

disease phenotype of APP/PS1 mice. *Neurobiol Aging*. 2016;40:22-40.

doi:10.1016/j.neurobiolaging.2015.12.021

67.   Hsu WCJ, Wildburger NC, Haidacher SJ, et al. PPARgamma agonists rescue increased

phosphorylation of FGF14 at S226 in the Tg2576 mouse model of Alzheimer's disease. *Exp Neurol*. 2017;295(Supplement C):1-17. doi:10.1016/j.expneurol.2017.05.005

68.   Reese LC, Zhang WR, Dineley KT, Kayed R, Taglialatela G. Selective induction of calcineurin activity and signaling by oligomeric amyloid beta. *Aging Cell*. 2008;7(6):824-835. doi:10.1111/j.1474-9726.2008.00434.x

69.   Comerota MM, Krishnan B, Taglialatela G. Near infrared light decreases synaptic vulnerability to amyloid beta oligomers. *Sci Rep*. 2017;7(1). doi:10.1038/s41598-017-15357-x

70.   Lasagna-Reeves CA, Castillo-Carranza DL, Guerrero-Muñoz MJ, Jackson GR, Kayed R. Preparation and characterization of neurotoxic tau oligomers. *Biochemistry*. 2010;49(47):10039-10041. doi:10.1021/bi1016233

71.   Comerota MM, Tumurbaatar B, Krishnan B, Kayed R, Taglialatela G. Near Infrared Light Treatment Reduces Synaptic Levels of Toxic Tau Oligomers in Two Transgenic Mouse Models of Human Tauopathies. *Molecular Neurobiology*. https://doi.org/10.1007/s12035-018-1248-9. Published 2018. Accessed September 12, 2018.

72.   Krishnan B, Kayed R, Taglialatela G. Elevated phospholipase D isoform 1 in Alzheimer's disease patients' hippocampus: Relevance to synaptic dysfunction and memory deficits. *Alzheimer's Dement Transl Res Clin Interv*. 2018;4:89-102. doi:10.1016/j.trci.2018.01.002

73.   Presley AD, Fuller KM, Arriaga EA. MitoTracker Green labeling of mitochondrial proteins and their subsequent analysis by capillary electrophoresis with laser-induced fluorescence detection. *J Chromatogr B Anal Technol Biomed Life Sci*. 2003;793(1):141-

150. doi:10.1016/S1570-0232(03)00371-4

74. Mattiasson G, Friberg H, Hansson M, Elmér E, Wieloch T. Flow cytometric analysis of mitochondria from CA1 and CA3 regions of rat hippocampus reveals differences in permeability transition pore activation. *J Neurochem*. 2003;87(2):532-544. doi:10.1046/j.1471-4159.2003.02026.x

75. Boucher J, Kleinridders A, Ronald Kahn C. Insulin receptor signaling in normal and insulin-resistant states. *Cold Spring Harb Perspect Biol*. 2014;6(1). doi:10.1101/cshperspect.a009191

76. Cao L, Wang Z, Wan W. Suppressor of cytokine signaling 3: Emerging role linking central insulin resistance and Alzheimer's disease. *Front Neurosci*. 2018;12(JUN):417. doi:10.3389/fnins.2018.00417

77. Ramlackhansingh AF, Brooks DJ, Greenwood RJ, et al. Inflammation after trauma: Microglial activation and traumatic brain injury. *Ann Neurol*. 2011;70(3):374-383. doi:10.1002/ana.22455

List of Abbreviations

Aβ – amyloid beta

aCSF – artificial cerebrospinal fluid

AD – Alzheimer's disease

AICD – amyloid precursor protein intracellular domain

APOE – apolipoprotein ε

APP – amyloid precursor protein

BACE-1 – beta-site amyloid precursor protein-cleaving enzyme 1

BBB – blood brain barrier

BCA – bicinchoninic acid

CNS – central nervous system

DPI – days post-injury

ELISA – enzyme-linked immunosorbent assay

FDA – Food and Drug Administration

fEPSP – field excitatory post-synaptic potentials

FPI – fluid-percussion injury

HBK – HEPES-buffered Krebs-like buffer

HFS – high frequency stimulation

IGF – insulin-like growth factor

IP – intraperitoneal

IR – insulin receptor

LTP – long-term potentiation

MAP – microtubule-associated protein

MCI – mild cognitive impairment

MPI – months post-injury

NFTs – neurofibrillary tangles

NMDAR - N-methyl-D-aspartate receptor

PMI – post-mortem interval

PSD – post-synaptic density

PS1 – presenilin 1

RCF – relative centrifugal force

ROS – reactive oxygen species

sAD – sporadic Alzheimer's disease

SOCS – suppressor of cytokine signaling

TBI – traumatic brain injury

T2DM – type 2 diabetes mellitus

WT – wild-type